Theses and Dissertations   1. Thesis and Dissertation Collection, all items

2005-09

Evaluation and selection of an efficient fuel/air initiation strategy for pulse detonation engines

Channell, Brent T.

Monterey California. Naval Postgraduate School

http://hdl.handle.net/10945/2026

NAVAL POSTGRADUATE SCHOOL

MONTEREY, CALIFORNIA

THESIS

EVALUATION AND SELECTION OF AN EFFICIENT FUEL/AIR INITIATION STRATEGY FOR PULSE DETONATION ENGINES

by

Brent T. Channell

September 2005

Thesis Advisor:	Christopher M. Brophy
Second Reader:	Jose O. Sinibaldi

Approved for public release; distribution is unlimited

THIS PAGE INTENTIONALLY LEFT BLANK

REPORT DOCUMENTATION PAGE	*Form Approved OMB No. 0704-0188*

Public reporting burden for this collection of information is estimated to average 1 hour per response, including the time for reviewing instruction, searching existing data sources, gathering and maintaining the data needed, and completing and reviewing the collection of information. Send comments regarding this burden estimate or any other aspect of this collection of information, including suggestions for reducing this burden, to Washington headquarters Services, Directorate for Information Operations and Reports, 1215 Jefferson Davis Highway, Suite 1204, Arlington, VA 22202-4302, and to the Office of Management and Budget, Paperwork Reduction Project (0704-0188) Washington DC 20503.

1. AGENCY USE ONLY *(Leave blank)*	2. REPORT DATE September 2005	3. REPORT TYPE AND DATES COVERED Master's Thesis	
4. TITLE AND SUBTITLE: Evaluation and Selection of an Efficient Fuel/Air Initiation Strategy for Pulse Detonation Engines		**5. FUNDING NUMBERS** N0001405WR20253	
6. AUTHOR(S) Brent T. Channell			
7. PERFORMING ORGANIZATION NAME(S) AND ADDRESS(ES) Naval Postgraduate School Monterey, CA 93943-5000		**8. PERFORMING ORGANIZATION REPORT NUMBER**	
9. SPONSORING /MONITORING AGENCY NAME(S) AND ADDRESS(ES) Office of Naval Research (ONR) Ballstone Tower One 800 N. Quincy St. Arlington, VA 22217-5660		**10. SPONSORING/MONITORING AGENCY REPORT NUMBER** N/A	

11. SUPPLEMENTARY NOTES The views expressed in this thesis are those of the author and do not reflect the official policy or position of the Department of Defense or the U.S. Government.

12a. DISTRIBUTION / AVAILABILITY STATEMENT Approved for public release; distribution is unlimited	12b. DISTRIBUTION CODE

13. ABSTRACT (maximum 200 words)

Rapid and efficient initiation of hydrocarbon/air mixtures has been identified as one of the critical and enabling technologies for Pulse Detonation Engines (PDEs). Although the NPS Rocket Propulsion Laboratory has successfully demonstrated fuel/air detonations in a valveless pulse detonation engine using ethylene, propane, and JP-10 fuels, past engine designs have relied upon a sensitive fuel/oxygen initiator unit. To realize the increased thermodynamic efficiencies of PDEs and thus compete with ramjets and other supersonic platforms, it is imperative to eliminate any need for supplementary oxygen in an air-breathing PDE design. This thesis examined ignition technologies and initiator designs which did not require auxiliary oxygen, including capacitive discharge systems and the developing technology of Transient Plasma Ignition (TPI).   The current NPS pulse detonation engine architecture was modified to evaluate the various ignition strategies in a PDE operating on an ethylene/air mixture at simulated supersonic cruising conditions. Comparisons were based upon ignition success rate, ignition delay time, detonation wave speed, and Deflagration-to-Detonation (DDT) distance. Reliability and performance of the TPI system proved to be superior to conventional ignition systems. Furthermore, successful initiation of a PDE operating at a frequency of up to 40 hertz was demonstrated without the use of supplementary oxygen.

14. SUBJECT TERMS Pulse Detonation Engines, PDE, PDE Ignition, PDE Initiation, Transient Plasma Ignition, TPI			**15. NUMBER OF PAGES** 71
			16. PRICE CODE
17. SECURITY CLASSIFICATION OF REPORT Unclassified	**18. SECURITY CLASSIFICATION OF THIS PAGE** Unclassified	**19. SECURITY CLASSIFICATION OF ABSTRACT** Unclassified	**20. LIMITATION OF ABSTRACT** UL

THIS PAGE INTENTIONALLY LEFT BLANK

EVALUATION AND SELECTION OF AN EFFICIENT FUEL/AIR INITIATION STRATEGY FOR PULSE DETONATION ENGINES

Brent T. Channell
Lieutenant Commander, United States Navy
B.S., University of Colorado, 1993

Submitted in partial fulfillment of the
requirements for the degree of

MASTER OF SCIENCE IN ASTRONAUTICAL ENGINEERING

from the

NAVAL POSTGRADUATE SCHOOL
September 2005

Author: Brent T. Channell

Approved by: Christopher M. Brophy
                 Thesis Advisor

                 Jose O. Sinibaldi
                 Co-Advisor

                 Anthony J. Healey
                 Chairman, Department of Mechanical & Astronautical Engineering

THIS PAGE INTENTIONALLY LEFT BLANK

ABSTRACT

Rapid and efficient initiation of hydrocarbon/air mixtures has been identified as one of the critical and enabling technologies for Pulse Detonation Engines (PDEs). Although the NPS Rocket Propulsion Laboratory has successfully demonstrated fuel/air detonations in a valveless pulse detonation engine using ethylene, propane, and JP-10 fuels, past engine designs have relied upon a sensitive fuel/oxygen initiator unit to initiate the less sensitive fuel/air mixtures. To realize the increased thermodynamic efficiencies of PDEs and thus compete with ramjets and other supersonic platforms, it is imperative to eliminate any need for supplementary oxygen in an air-breathing PDE design. This thesis examined ignition technologies and initiator designs which did not require auxiliary oxygen, including capacitive discharge systems and the developing technology of Transient Plasma Ignition (TPI). The current NPS pulse detonation engine architecture was modified to evaluate the various ignition strategies in a PDE operating on an ethylene/air mixture at simulated supersonic cruising conditions. Comparisons were based upon ignition success rate, ignition delay time, detonation wave speed, and Deflagration-to-Detonation (DDT) distance. Reliability and performance of the TPI system proved to be superior to conventional ignition systems. Furthermore, successful initiation of a PDE operating at a frequency of up to 40 hertz was demonstrated without the use of supplementary oxygen.

THIS PAGE INTENTIONALLY LEFT BLANK

TABLE OF CONTENTS

THIS PAGE INTENTIONALLY LEFT BLANK

LIST OF FIGURES

THIS PAGE INTENTIONALLY LEFT BLANK

LIST OF TABLES

THIS PAGE INTENTIONALLY LEFT BLANK

ACKNOWLEDGMENTS

The author would like to express his profound gratitude to Professor Christopher Brophy and Professor Jose Sinibaldi for the help, guidance, and education they provided while pursuing this thesis work. Their clear dedication to both the research profession and education was admired and appreciated.

The author would also like to thank Mr. George Hageman for his extensive work, technical expertise, and enthusiasm at the Rocket Propulsion Lab. The support of our sponsors at the Office of Naval Research was also appreciated, and the efforts of our colleagues at the University of Southern California, particularly Mr. Fei Wang, Mr. Charles Cathey, and Professor Martin Gundersen, were invaluable.

Finally, the author would like to express his deep gratitude to the support of his wife, Beth, in this and all endeavors.

THIS PAGE INTENTIONALLY LEFT BLANK

I. INTRODUCTION

While the technology of Pulse Detonation Engines (PDE) has made great advances in the past twenty years, the idea of using intermittent detonations to produce thrust can be traced back to the work of Hoffman in Germany in the late 1930s [1]. Recently, there has been renewed interest in the technology for application to supersonic propulsion. A recent study by Harris, et al. found the specific impulse of a PDE to range from 36% higher than a ramjet at Mach 1.5 to 4% greater at Mach 5 [2]. While the specific numbers vary from study to study, Figure 1 presents the performance of different propulsion concepts in terms of their relative specific impulse and Mach number regimes.

Turbojets and turbofans offer significantly superior specific impulse at subsonic and low supersonic flight velocities, but are structurally and thermodynamically limited to about Mach 3-4 due to the compressor discharge conditions at high flight velocities. Ramjets and scramjets are capable of higher speeds, but without the added compression of the incoming air by a compressor their specific impulse suffers due to the lower Brayton cycle efficiencies. Additionally, these engines must be boosted to the supersonic velocities at which they can operate. Due to these limitations, most short-range supersonic tactical missiles have been powered by solid rocket motors, which have the lowest specific impulse, but are the simplest in design and operate over the widest velocity range. Long-range missiles and aircraft take advantage of the high fuel-based specific impulse of turbojets and turbofans, but have associated higher costs and flight Mach number limitations. The PDE is envisioned as an alternative for the ramjet and a low-cost substitution for expendable gas turbine systems to bridge the gap in propulsion technology. With specific impulses exceeding 2000 seconds, and a design that can be accelerated from subsonic to supersonic, PDEs may propel missiles, aircraft and possibly some combined-cycle launch vehicles.
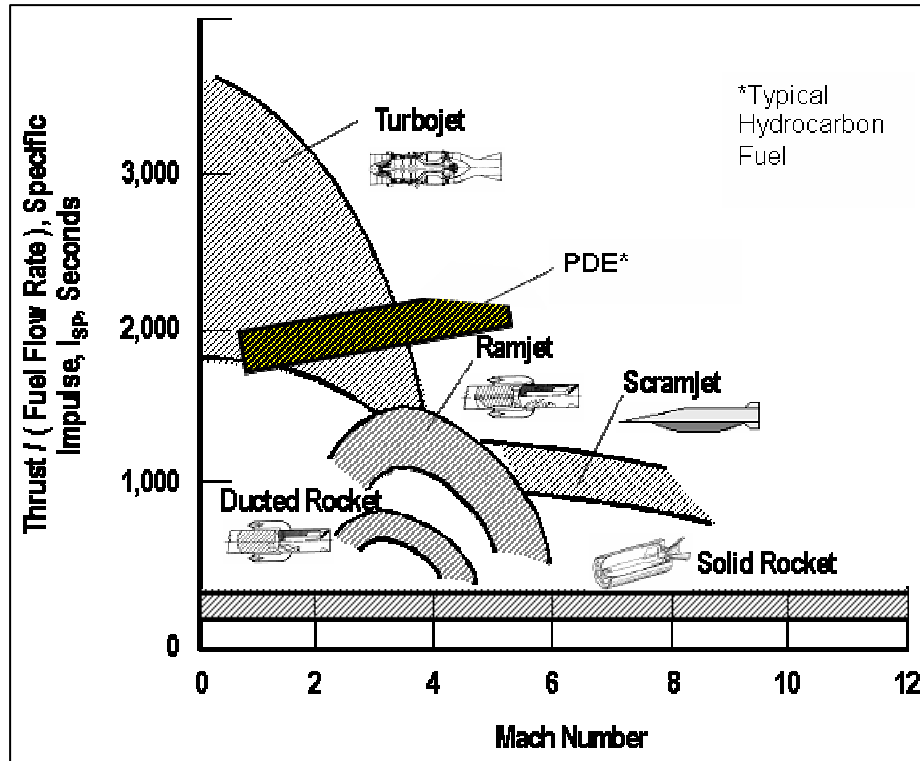
Figure 1.   Comparison of High-Speed Propulsion Technologies (After Ref. 3)

PDEs operate by initiating a detonation wave that propagates through a combustor filled with a fuel-air mixture. The detonation wave inherently creates considerable chamber pressures without the moving machinery of a compressor or turbine and produces thrust by expanding the combustion products at the aft end of the combustor [4]. If the detonation process is repeated at a high enough frequency, the result is near-constant thrust. A PDE takes advantage of the fact that a detonation event approximates a constant volume combustion process, which has much greater thermodynamic efficiency than a constant pressure combustion process used in a Brayton cycle. Thus, due to its relatively simple design with no moving machinery and enhanced thermodynamic efficiency, the PDE has become an attractive propulsion alternative.

Past research at the Naval Postgraduate School Rocket Propulsion Lab has demonstrated successful PDE designs fueled by ethylene, propane, or JP-10. However, many of the previous designs have relied upon a fuel/oxygen initiator to start the detonation wave propagation in a fuel/air mixture. The initiator was a small combustion

chamber within the main chamber, in which fuel was mixed with oxygen. The result was a highly sensitive mixture that was relatively easy to detonate repeatedly and reliably. The current work focused on initiating detonation waves without an initiator and therefore without the need for supplementary oxygen. Removing these constraints simplifies the design, and more importantly, increases the performance of the PDE in terms of specific impulse. Fuel-based specific impulse is defined as the thrust per unit weight of fuel delivered by an engine, as shown in Equation (1). Although supplementary oxygen is obviously an oxidizer, it would be considered a fuel in this calculation because the flight vehicle would be required to carry the oxygen required for the initiator operation. Eliminating the initiator fuel and oxygen terms in the denominator, and designing a PDE that only relies on air for an oxidizer, would then increase the performance of the engine, making it a competitor against the ramjet in terms of fuel-based specific impulse.

$$I_{sp_f} = \frac{F}{\dot{m}_{fuel} g} = \frac{F}{(\dot{m}_{fuel} + \dot{m}_{fuel\_init} + \dot{m}_{O_2}) g} \qquad (1)$$

THIS PAGE INTENTIONALLY LEFT BLANK

II.   BACKGROUND

A.   DETONATION THERMODYNAMICS

1.   Character and Structure of Detonation Waves

A review of the theory and thermodynamics of detonations is required to explain how a PDE system gains the benefits described earlier.   Since a PDE relies on a detonative combustion mode, it is important to understand the differences between a deflagration and detonation combustion process.   Both processes require a reactive mixture which permits rapid energy release to sustain the combustion wave. Whether the mixture supports a detonation or a deflagration depends upon certain conditions, including the ignition source, the fuel/air mixture ratio, and the surrounding confinement [5].   When the conditions result in a subsonic combustion wave, it is considered a deflagration, which occurs at nearly constant pressure. Most combustion processes are deflagrations, from the burning of a candle to the combustion inside a turbojet.   A detonation wave, however, is a supersonic combustion wave. Glassman precisely defined it as "a shock wave that is sustained by the energy of the chemical reaction in the highly compressed explosive medium existing in the wave" [5]. Note that a detonation is not the same as an explosion. An explosion is indeed a rapid heat release or pressure rise, but it does not require the existence of a combustion wave.

A one-dimensional (1D) planar model of a combustion wave is depicted in Figure 2. Actual combustion processes have complex three-dimensional structures, but the 1D model is used to demonstrate the basic properties. In this model's frame of reference, the combustion wave is considered as stationary.   Thus, the unburned gases travel into the wave at a velocity of u_1 and the burned gases travel out of the wave at a velocity of u_2. Referring to the nomenclature of Figure 2, the fundamental differences between detonation and deflagration are illustrated in Table 1.
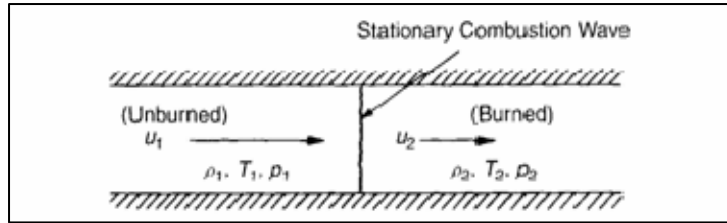
Figure 2.   Stationary One-Dimensional Combustion Wave (From Ref. 6)

	Detonation	Deflagration
u_1/c_1	5-10	0.0001-0.03
u_2/u_1	0.4-0.7 (deceleration)	4-16
p_2/p_1	13-55 (compression)	0.98-0.976 (slight expansion)
T_2/T_1	8-21 (heat addition)	4-16 (heat addition)
ρ_2/ρ_1	1.4-2.6	0.06-0.25

Table 1.   Qualitative Differences between Detonation and Deflagration (After Ref. 5, 6)

As previously mentioned, u_1/c_1, or the local Mach number, is supersonic for detonation and subsonic for deflagration. Both processes add heat to the mixture, but the shock wave that results from detonation greatly compresses the reactants and produces high temperature and pressure products, which can then be accelerated to generate thrust. Another characteristic difference between detonation and deflagration is the relative velocity u_2/u_1. For deflagration, the burned reactants accelerate away from the combustion wave. However, the reactants decelerate after passing through a detonation wave. In another frame of reference in which the combustion wave is moving into stationary unburned reactants, the burned reactants move away from a passing deflagration wave but move *towards* a detonation wave. This frame of reference is illustrated in Figure 3.
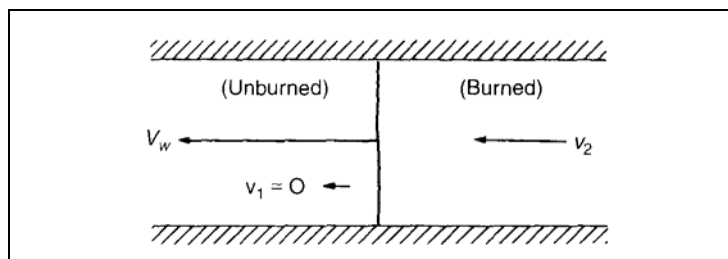
Figure 3.   Detonation Wave in the Laboratory Coordinate System (From Ref. 6)

6

The speed at which the burned reactants travel towards a detonation wave was an area of extensive study for two separate researchers, Chapman and Jouguet, around the turn of the 20th century. The starting point for their derivations began with the conservation equations for steady, one-dimensional flow in a constant area duct:

Continuity equation: $\rho_1 u_1 = \rho_2 u_2$ (2)

Conservation of momentum: $p_1 + \rho_1 u_1^2 = p_2 + \rho_2 u_2^2$ (3)

Conservation of energy: $c_p T_1 + \dfrac{1}{2} u_1^2 + q = c_p T_2 + \dfrac{1}{2} u_2^2$ (4)

Equations (2) through (4) can be arranged to result in the Hugoniot Relation[1], which relates the heat release per unit mass, or heat transferred into the system, q, to the pressures and densities of the burned and unburned reactants:

$$\frac{\gamma}{\gamma - 1}\left(\frac{p_2}{\rho_2} - \frac{p_1}{\rho_1}\right) - \frac{1}{2}(p_2 - p_1)\left(\frac{1}{\rho_1} + \frac{1}{\rho_2}\right) = q$$ (5)

Two equivalent forms of the Hugoniot Relation associate the total enthalpy, h, or the total internal energy, e, to the pressures and densities of the products and unburned reactants:

$$\frac{1}{2}(p_2 - p_1)\left(\frac{1}{\rho_1} + \frac{1}{\rho_2}\right) = h_2 - h_1$$ (6)

$$\frac{1}{2}(p_2 + p_1)\left(\frac{1}{\rho_1} - \frac{1}{\rho_2}\right) = e_2 - e_1$$ (7)

Using Equation (5), a curve that describes the thermodynamic conditions of combustion, called the Hugoniot curve, may be constructed. For a given q and values of $(1/\rho_1, p_1)$, the Hugoniot curve plots the possible values of $1/\rho_2$ versus p_2.

---

[1] The derivation of the Hugoniot relation is treated equally well in Glassman [5] and Kuo [6].
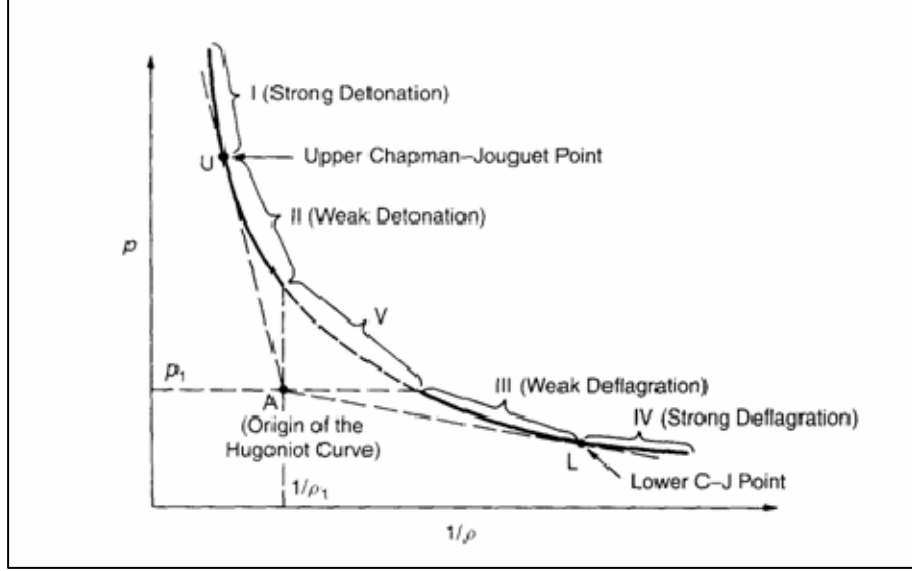
Figure 4.   Hugoniot Curve with Solution Regions (From Ref. 6)

Mathematically, there are five possible solution regions on the Hugoniot curve, as seen in Figure 4. They are divided by a constant pressure line, a constant specific volume line, and tangent lines drawn from the origin of the Hugoniot curve. These tangent lines intersect the curve at the upper and lower Chapman-Jouguet (C-J) points, U and L. However, it must be noted that not all of the regions are physically observed. Region V is not possible, as it requires $p2 > p1$ and $1/\rho_2 > 1/\rho_1$, which would result in an imaginary velocity of u_1 in the Rayleigh-line relation, Equation (8):

$$\rho_1^2 u_1^2 = \frac{p_2 - p_1}{1/\rho_1 - 1/\rho_2} = \dot{m}^2 \tag{8}$$

Regions I and II are rarely observed and would be transient in nature. Region I, termed the strong detonation region because $p_2 > p_U$, requires an overdriven shock. Region II, the weak detonation region, requires very fast chemical kinetics. Region IV, the strong deflagration region, is not possible in a constant area duct. In this region, the gas velocity relative to the wave front must accelerate from subsonic to supersonic, which violates Rayleigh flow. Thus, the physically possible solutions to the Hugoniot curve are only region III, weak deflagration, and the upper C-J point, U, which is the unique solution for C-J detonations.

8

An important result was discovered upon differentiating and rearranging the Hugoniot relation, which gives the slope of the curve:

$$\frac{dp_2}{d(1/\rho_2)} = \frac{(p_2 - p_1) - \left(\frac{2\gamma}{\gamma-1}\right)p_2}{\left(\frac{2\gamma}{\gamma-1}\right)\frac{1}{\rho_2} - \left(\frac{1}{\rho_1} + \frac{1}{\rho_2}\right)} \tag{9}$$

However, the slope at the C-J points can also be written as

$$\frac{dp_2}{d(1/\rho_2)} = \frac{p_2 - p_1}{1/\rho_2 - 1/\rho_1} \tag{10}$$

Therefore, by equating Equations (9) and (10), and combining the result with the Rayleigh-line relation, Equation (8), the solution is the velocity of the burned reactants following a detonation:

$$u_2^2 = \frac{\gamma p_2}{\rho_2} = c_2^2 \tag{11}$$

That is, the burned reactants travel at the local speed of sound relative to the detonation wave.

Further, at the upper C-J point, $1/\rho_2 < 1/\rho_1$, it follows from the Rayleigh line relation that $u_1 > u_2$; that is, u_1 is supersonic. Translating this to the laboratory frame of reference, as in Figure 3, the detonation wave speed, V_w, is supersonic. Thus, the burned reactants will not catch the detonation wave, although they are moving in the same direction.

As the shock wave of a detonation passes through a fuel-air mixture, the mixture becomes highly compressed and heated. Traveling just behind the shock wave is the flame front of the combustion wave. Upon the flame's arrival, an extremely energetic chemical reaction occurs within the compressed mixture, which in turn sustains the shock wave. This explanation of a detonation event was first theorized independently by Zeldovich, von Neumann, and Doring. Presented in Figure 5 is what has become known as the ZND model of a one-dimensional detonation wave.
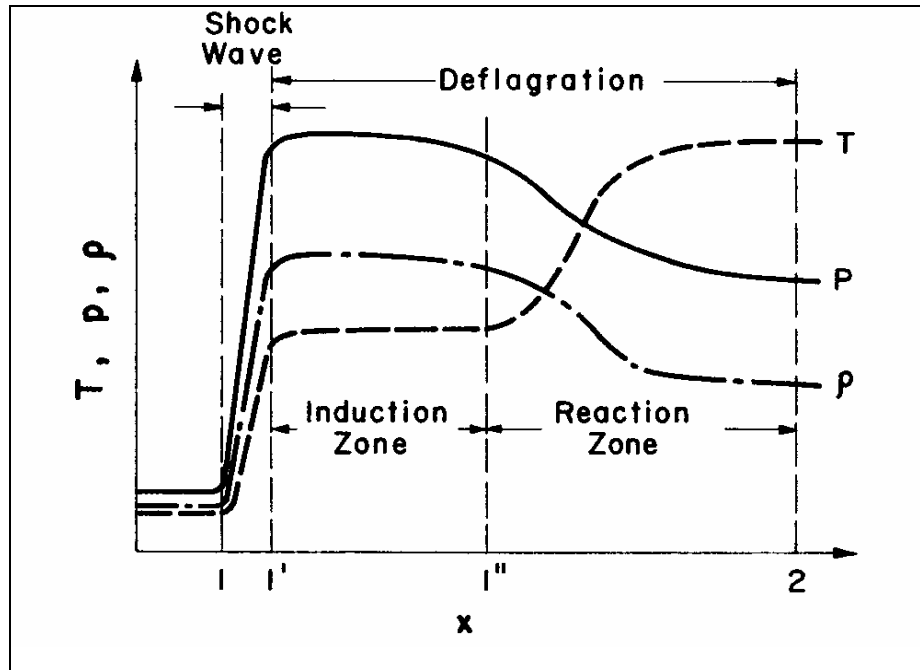
Figure 5.   ZND One-Dimensional Wave Structure (From Ref. 6)

As seen in the ZND model, the pressure, density, and temperature sharply rise as the relatively-thin, planar shock wave passes through the mixture at the detonation wave speed. Followed immediately by a region called the induction zone, the thermodynamic properties remain comparatively constant until the arrival of the reaction zone. At that point, the properties quickly change as energy is released in the rapid chemical reaction.

While the ZND model accurately describes the process in one dimension, the chemical reaction directs energy in all directions and not just towards the leading shock wave. Thus, actual detonation waves have a complex three-dimensional structure. The leading shock is a normal shock wave, but not completely planar. The normal segments are curved and intersected by lateral shock waves, creating triple points which produce a distinctive fish-scale pattern on the surface of the confining media. This characteristic pattern has been captured by smoked-foil records and an example is shown in Figure 6. The triple points, where three shock waves intersect, create areas of intense pressure and temperature.
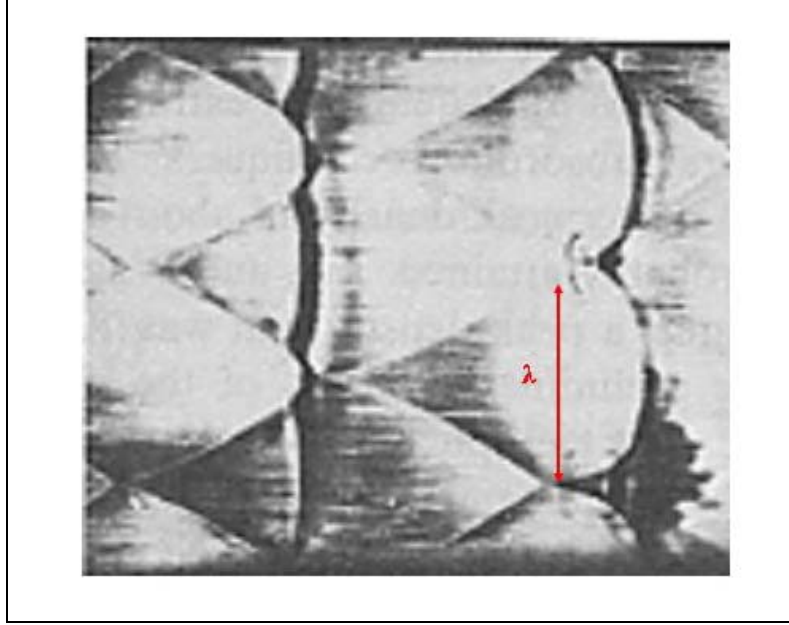
Figure 6.   Three-Dimensional Detonation Wave Structure (After Ref. 6)

Annotated in Figure 6 is the dimension λ, called the cell size, which is indicative of the sensitivity of a mixture and is of particular importance in detonation applications. Highly sensitive mixtures, which are easily detonable, typically have a smaller cell size, as it is related to the size of the induction zone described in the ZND model. Further, there is a critical tube diameter, d_c, which will allow a detonation wave to continue as a spherical wave when it transitions from the end of the tube to an unconfined space containing the same mixture. The critical diameter has been empirically determined to be $d_c \approx 13\lambda$ [5, 7]. Additionally, there is a constraint called the quenching diameter, which is associated to the growth of the boundary layer within the tube. (Thus, it is related to the Reynolds number and cell size). A detonation wave will not propagate in a tube smaller than the quenching diameter.

2.   Comparison of Detonation and Constant Pressure Cycles

One of the primary motivations for utilizing detonation waves for propulsion is the substantial gain in thermal efficiency over combustion methods that employ the Brayton cycle, such as turbojets and ramjets. To illustrate this benefit, the two thermodynamic cycles were compared for a theoretical propulsion system operating at

supersonic cruise conditions at an altitude of 16,200 meters. At that height, the ambient conditions of approximately 0.1 bar and 216.6 K were used as the pressure and temperature of State 0. In this scenario, both cycles used a mixture of ethylene and air at an equivalence ratio of 1.1. The fuel/air mixture then experienced isentropic compression in both cycles to arrive at State 1. State 2 followed either constant-pressure combustion or detonation, depending upon the cycle, followed by isentropic expansion to arrive at State 4.

The software Cequel (Chemical Equilibrium in Excel), produced by Software Engineering Associates in Carson City, Nevada, was employed at these conditions to calculate the working fluid's temperature, density, entropy and molecular weight at each stage in the respective thermodynamic cycle. Further, the ratio of specific heats (γ) was computed at each state, but they were assumed to be constant from States 0 to 1 and States 2 to 4. The results of the cycle analysis are summarized in Table 2 and illustrated as pressure versus specific volume (p-v) plots in Figures 7 and 8.

Constant Pressure (Brayton) Combustion Cycle

State	Pressure (bar)	Temp (K)	Specific Volume (m^3/kg)	Entropy (kJ/(kg K))
0	0.1	216.6	5.344	6.337
1	1	294.2	0.744	6.337
2	1	2372.7	7.002	9.724
4	0.1	1536.1	45.063	9.724

C-J Detonation Cycle

State	Pressure (bar)	Temp (K)	Specific Volume (m^3/kg)	Entropy (kJ/(kg K))
0	0.1	216.6	5.344	6.337
1	1	294.2	0.744	6.337
2	19.1	2966.9	0.466	9.307
4	0.1	1131.8	33.201	9.307

Table 2.   Comparison of Constant Pressure and Detonation Cycles
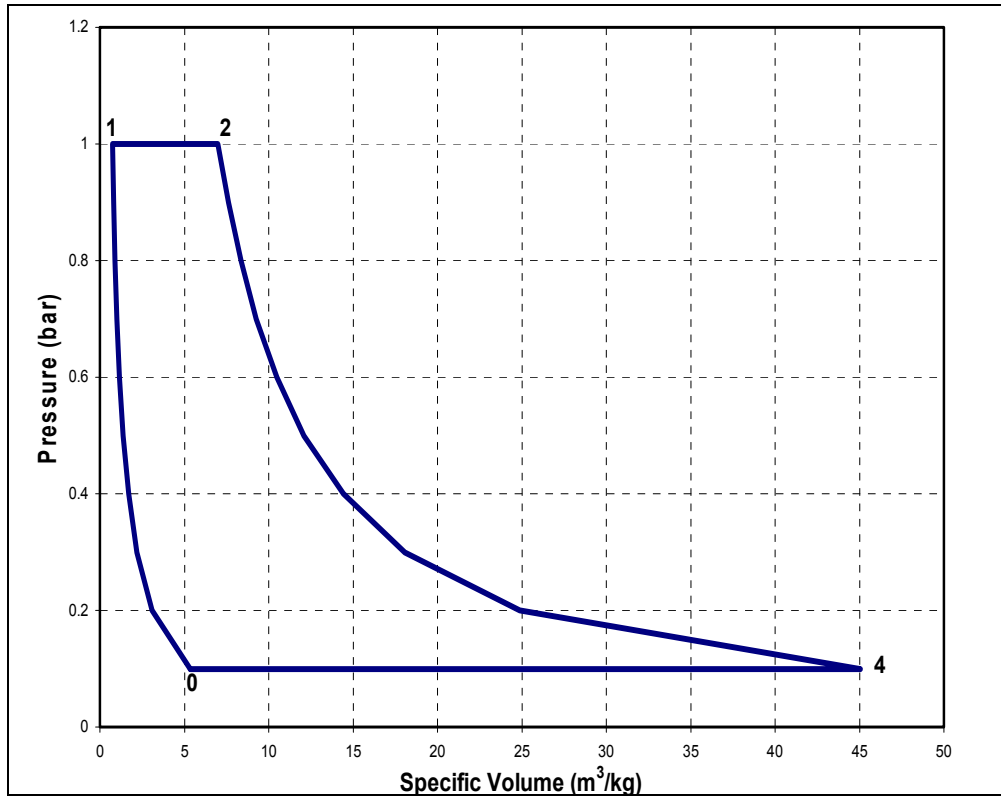
Figure 7.   Constant Pressure (Brayton) Combustion Cycle
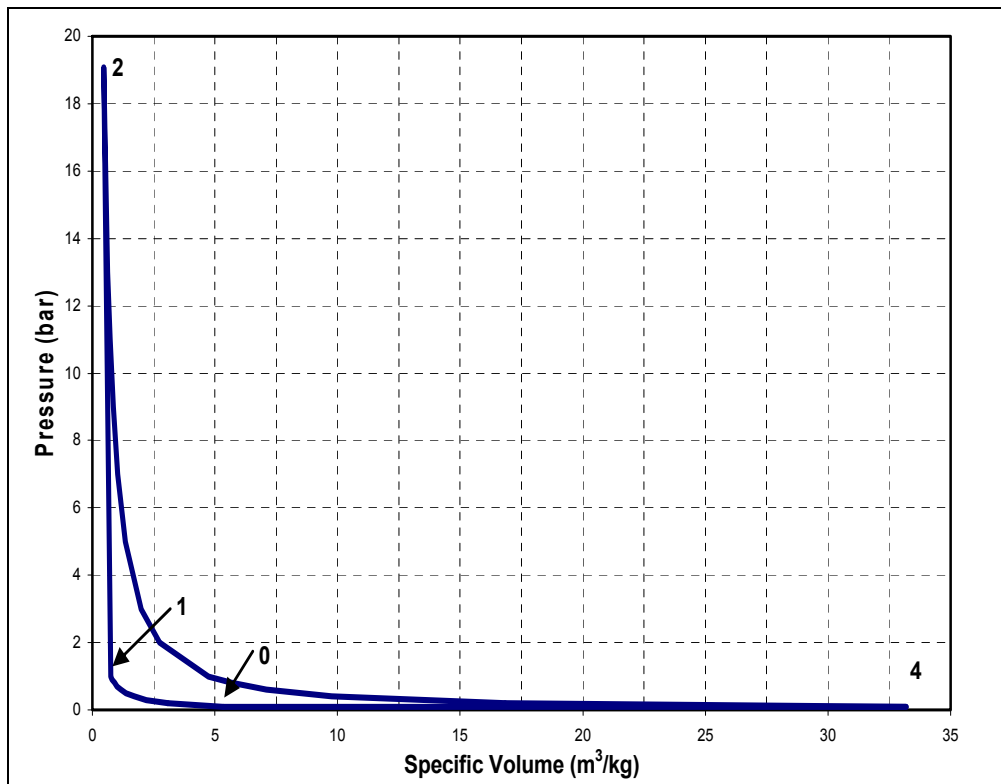

Figure 8.   C-J Detonation Cycle

13

The results in Table 4 show that the change in entropy was 12.3% less for the detonation cycle. A smaller entropy rise implies the system has greater capacity for useful work. To examine this difference further, the net work of a thermodynamic cycle can be determined by integrating the area enclosed by its p-v plot. Equation (12) represents the constant pressure cycle while the detonation cycle is represented by Equation (13):

$$
\begin{aligned}
w_{Brayton} &= p_1(v_2 - v_1) + \int_2^4 pdv - \int_0^1 pdv - p_0(v_4 - v_0) \\
&= p_1(v_2 - v_1) + \frac{(p_1v_1 - p_0v_0)}{1 - \gamma_{0-1}} + \frac{(p_4v_4 - p_2v_2)}{1 - \gamma_{2-4}} + p_0(v_0 - v_4)
\end{aligned}
\tag{12}
$$

$$
\begin{aligned}
w_{C-J} &= \int_2^4 pdv - \int_0^1 pdv - p_0(v_4 - v_0) \\
&= \frac{p_1v_1 - p_0v_0}{1 - \gamma_{0-1}} + \frac{1}{2}\left(\frac{p_2 - p_1}{v_2 - v_1}\right)\left(v_2^2 - v_1^2\right) \\
&+ \left[p_2 - \left(\frac{p_2 - p_1}{v_2 - v_1}\right)v_2\right](v_2 - v_1) + \frac{p_4v_4 - p_2v_2}{1 - \gamma_{2-4}} + p_0(v_0 - v_4)
\end{aligned}
\tag{13}
$$

Once the net work of a system is determined, the thermodynamic efficiency can be found by dividing the net work by the heat added to the system:

$$
\eta = \frac{w}{q_H}
\tag{14}
$$

For the constant-pressure cycle, the added heat is calculated by Equation (15):

$$
q_{H_B} = c_{p2}T_2 - c_{p1}T_1
\tag{15}
$$

where c_{p2} is defined as $c_p = \left(\frac{\gamma R}{\gamma - 1}\right)$
\hfill (16)

For the detonation cycle, the added heat is found by Equation (17):

$$
q_{H_{CJ}} = \frac{(u_2 - c_2)^2}{2} + c_{p2}T_2 - c_{p1}T_1 - \frac{u_2^2}{2}
\tag{17}
$$

where u_2 is the velocity of the detonation wave and c_2 is the local speed of sound, both of which were calculated by Cequel.

14

Table 3 summarizes the results of these calculations for the constant-pressure and detonation cycles. As expected, the smaller entropy rise in the detonation cycle corresponded to more net work. Additionally, less heat went into the detonation cycle. These two contributing factors resulted in 21% higher thermodynamic efficiency over the constant pressure cycle. Of course, the calculated efficiencies are higher than actual values due to the stated assumptions, such as isentropic compression and expansion as well as adiabatic processes. However, the relative differences remain valid.

	Entropy Change (kJ/(kg K))	Heat Addition (kJ/kg)	Net Work (kJ/kg)	Efficiency η_{th} (%)
Constant Pressure	3.39	3063.5	1127.3	36.8
Detonation	2.97	2501.3	1446.5	57.8

Table 3.   Summary of Thermodynamic Cycle Comparison

3.   Effect of Inlet Diffuser Efficiency

All air-breathing engines benefit from maximizing pressure recovery at the engine inlet, or inlet efficiency, which will increase the overall thermal efficiency of a PDE. First, note that the efficiency of any fixed inlet will vary depending upon the flight Mach number. One standard pressure recovery schedule, MIL-E-5007D, is shown in Figure 9. In this schedule, the inlet efficiency is given by Equation (18):

$$\eta_I = \frac{P_{T1}}{P_{T0}} \tag{18}$$

where P_{T1} is the total pressure entering the combustion chamber and is a function of altitude and Mach number; P_{T0} is the total pressure entering the inlet under isentropic conditions, and is also a function of altitude and Mach number.
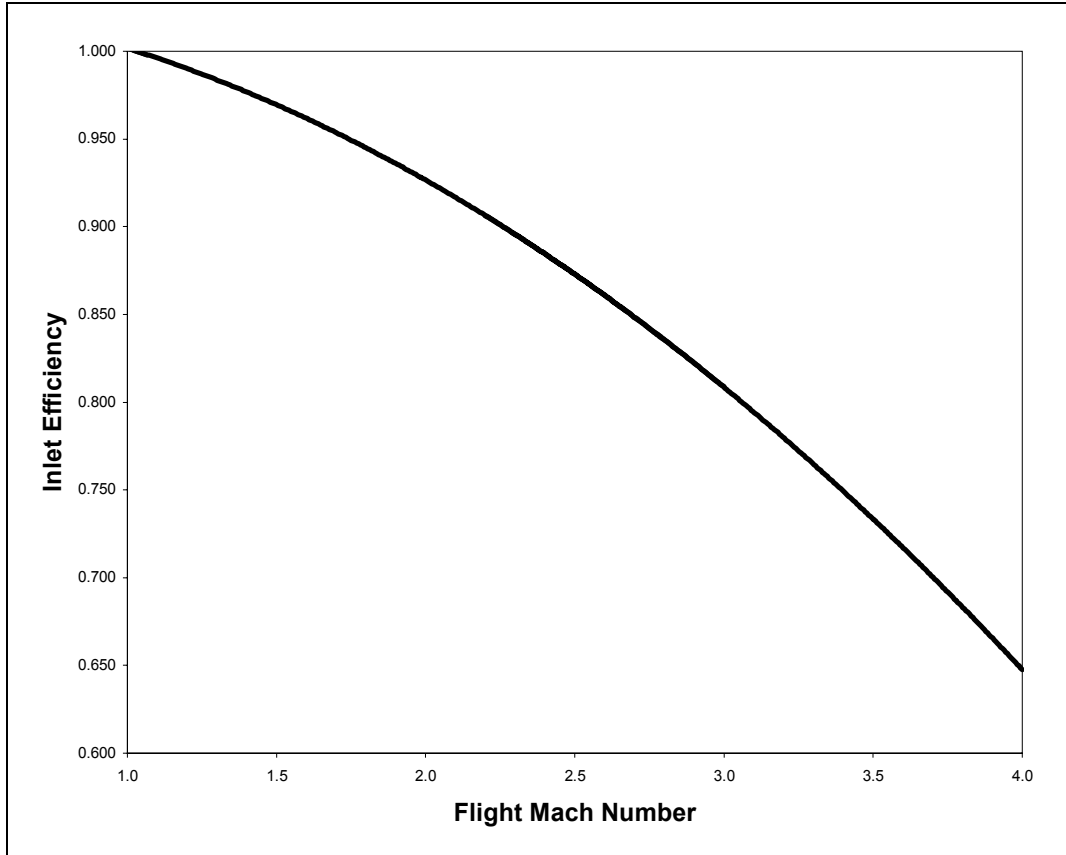
Figure 9.　　Inlet Efficiency based upon MIL-E-5007E Pressure Recovery

The same hypothetical Brayton cycle engine and PDE combustion cycle used in the previous section will be used to compare the two thermodynamic cycles with varying inlet efficiencies at a flight Mach number of 2.16. To begin, supersonic diffuser efficiency is defined by the total pressure entering and leaving the diffuser and is dependent upon the Mach number, as given by Equation (19) [8]:

$$\eta_I = \frac{\left(\dfrac{p_1}{p_0}\right)^{\frac{\gamma-1}{\gamma}} - 1}{\dfrac{\gamma-1}{2}M_0^2} \tag{19}$$

Rearranging this equation to solve for p_1, the total pressure leaving the diffuser, results in Equation (20):

16

$$p_1 = p_0 \left(\frac{\gamma - 1}{2} M_0^2 \eta_I + 1 \right)^{\frac{\gamma}{\gamma-1}} \tag{20}$$

The resultant pressure was then used as the pre-combustion pressure at State 1 in the thermodynamic cycles explained above. Then, for the given pressure of 0.1 bar at State 0 and flight Mach number of 2.16, the effect of varying the diffuser efficiency was analyzed. As shown in Figure 10, the detonation cycle maintains its advantage in thermal efficiency as inlet efficiency is reduced. In fact, the benefit slightly increases with declining inlet efficiency. At an inlet efficiency of 60%, the thermal efficiency of the detonation cycle is 23.6% higher than the constant pressure cycle. Referring again to Figure 9, if the engine inlet was designed to conform to MIL-E-5007E, an inlet efficiency of 91% would be expected at Mach 2.16. At this inlet efficiency, the detonation cycle would have a thermal efficiency 21.6% higher than that of the constant pressure cycle.
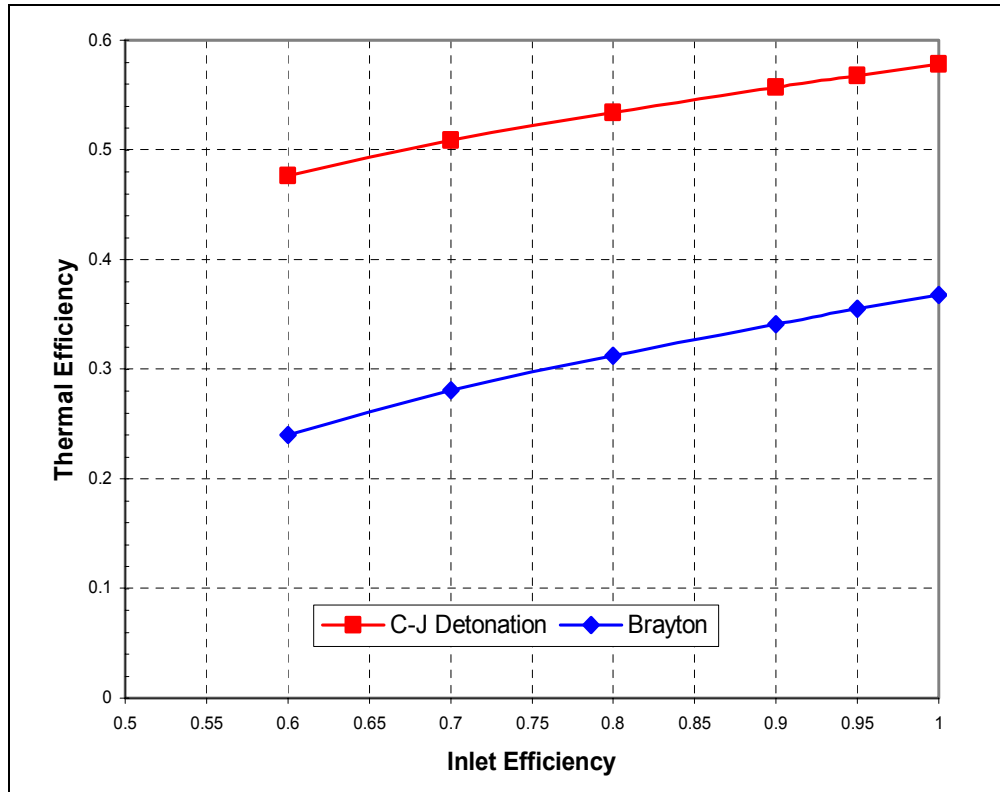

Figure 10.   Thermal Efficiency vs Inlet Efficiency

B.   PDE DESIGN AND OPERATING CYCLE

PDEs are constructed around two differing conceptual designs which relate how air is delivered to the combustion chamber of an engine. Valved PDEs utilize a valve mechanism to deliver and isolate the air into the combustion chamber, precisely timing it with fuel injection and ignition. Valveless PDEs allow air to continuously flow through the engine, timing only the fuel injection and ignition.

The NPS PDE architecture is based upon a valveless design, and the operating cycle has six steps as shown in Figure 11. The cycle begins with air flowing through the engine, purging the combustion products from the previous cycle. Fuel is then injected into the air flow and a fuel/air mixture begins to enter the combustion chamber at the head end. After filling the length of the combustion chamber with the fuel/air mixture, the ignition system is triggered in step 3.   Step 4 shows the combustion event transitioning to a detonation wave. The processes by which detonation is initiated are varied and are explained in a following section. The detonation wave travels the remaining length of the tube, leaving high pressure combustion products behind it. After the detonation wave exits the open end of the tube in step 5, the combustion products suddenly "sense" atmospheric pressure, allowing a rarefaction wave to propagate upstream and lower the chamber pressure to atmospheric pressure. The rarefaction wave travels to the head end in step 6, relieving the engine of high pressure and combustion products. The cycle then continues again with fresh air flowing through the engine and purging any remaining products.

1. Continuous air flow
2. Fuel/air mixture enters
6. Expansion wave travels
   length of tube
3. Ignition event
5. Expansion waves enter
4. Combustion transitions
   to detonation

Air flow   Fuel/Air mix   Combustion products
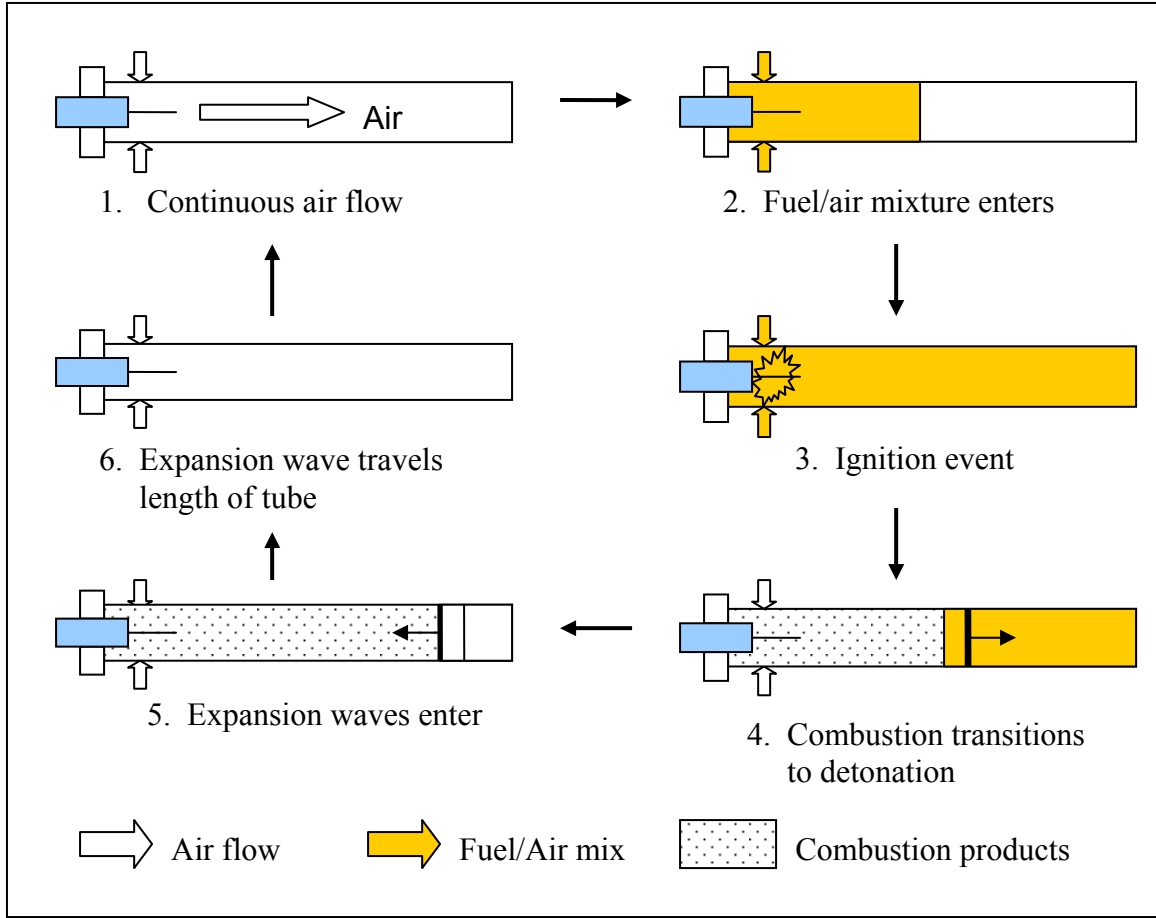
Figure 11.   Valveless PDE Cycle

C.   HIGH FREQUENCY OPERATION

The operating cycle outlined above must be repeated as often and quickly as possible to generate quasi-steady thrust. Thrust levels for practical systems require repetition rates above 60 Hz, and this introduces additional considerations. The first factor is the minimization of the t_{fill} and $t_{ignition\_delay}$ portions of the cycle, represented by Equation 21:

$$t_{cycle} = t_{fill} + t_{ignition\_delay} + t_{detonation} + t_{blowdown} + t_{purge} \qquad (21)$$

The time required to fill the combustion tube with the fuel/air mixture is dictated by the volume of the tube and the mass flow rate into the combustor. Thus, the engine geometry and injection strategy are foremost considerations. The length and diameter of the combustion tube determines the fill volume, while the fill rate is dependent upon the

diameter as well as the mass flow rate of the fuel/air mixture. The mass flow rate of air is in turn dependent upon flight velocity, altitude, and inlet capture area.

Minimizing the detonation initiation time and transition distance will not only reduce the cycle time, but also leads to shorter combustion tubes. Hence, fill time could be reduced. Blowdown and purge time is the cumulative time that the detonation wave completes its passage followed by the expansion waves entering the tube and clearing the combustion products prior to the next cycle. The continuous air flow of a valveless PDE design inherently decreases the purge time as it aids in clearing the tube.

A particular challenge in high frequency operations is optimizing the ignition timing with the fuel valve timing, and ensuring these operations do not overlap with the previous cycle. If a new fuel/air mixture enters the chamber prior to completion of the previous purge, reactants and combustion products would be mixed, altering the fuel/air ratio, possibly pre-igniting the next cycle, and decreasing the average thrust of the engine.

Finally, the thrust of a PDE is directly related to the momentum flux from the open end of the combustion tube. When the detonation wave exits the tube, allowing expansion waves to enter, the total pressure within the tube may fall below ambient pressure. Therefore, it is essential to couple consecutive cycles as closely as possible to alleviate this effect. Again, the continuous airflow of a valveless PDE will also help by preventing the chamber pressures from falling below the local ambient pressure.

III. EXAMINATION OF INITIATION STRATEGIES

The focus of this thesis work was on selecting the most favorable initiation strategy to incorporate into the NPS PDE architecture which would eliminate the dependence upon an initiator with supplementary oxygen. Detonations can be generated by one of three methods: direct initiation, shock focusing, or deflagration-to-detonation transition (DDT). This work concentrated on DDT techniques, but also compared the emerging technology of Transient Plasma Ignition (TPI) to more traditional capacitive discharge ignition systems. Finally, screens with varied mesh sizes were tested at the inlet of the combustion tube to evaluate the effects of flow conditioning and different turbulence length scales.

A. DETONATION INITIATION

1. Direct Initiation

Direct initiation relies upon a minimum critical energy release to directly produce a detonation wave. This can be accomplished by an explosive charge or the focusing of high-powered, pulsed laser energy. Both techniques, however, are impractical in PDE applications due to explosion containment as well as mass and power constraints.

2. Shock Focusing

The method of shock focusing uses the reflections of a shock wave, or multiple shock waves, to create high pressure and temperature regions. Focusing may be achieved by combustor geometry, turbulence devices, or injection jets. In a combustible mixture, a detonation can result from generating multiple hot spots. This method is extremely dependent upon geometry to focus moderately strong shocks. Thus, in the highly dynamic environment of a multiple-cycle PDEs, it has only had limited success.

3. Deflagration-to-Detonation Transition

The bulk of this work relied upon deflagration-to-detonation transition. DDT is the manner in which a laminar flame, or deflagration, becomes a detonation wave. When a combustible mixture within a tube is ignited, a kernel is initially generated which grows into a laminar flame and quickly becomes a wrinkled, turbulent flame. The combustion of the turbulent flame produces compression waves ahead of the flame, which coalesce

and form a shock front. The flame, which was already wrinkled, breaks into a turbulent brush due to the gas movement that was stimulated by the shock. The turbulent flame has increased surface area, which in turn increases its reaction and energy release rates. This continues until an "explosion within an explosion" occurs, creating two shocks: a forward traveling shock, called a superdetonation, and a backward traveling shock, or retonation. A spherical shock is also produced, creating lateral shock waves that interact with the superdetonation and retonation waves. Finally, after a progression of shock interaction, a self-sustaining detonation wave will form [6].

Turbulence generating devices are frequently inserted into the tube to accelerate the DDT process and consequently shorten the required length of the combustion tube. The devices are intended to enhance the shock-generated turbulence and increase the flame surface area, while also creating more shock reflections. Different devices include orifice plates, bolts, or spirals.

B.   CAPACITIVE DISCHARGE VS. TRANSIENT PLASMA IGNITION

In association with Professor Gundersen's group at the University of Southern California, the NPS Rocket Propulsion Lab is studying Transient Plasma Ignition (TPI) as an alternative to Capacitive Discharge Spark Ignition (CDSI) systems for PDEs. TPI employs a pseudo-spark or corona discharge that occurs on a time scale in the tens of nanoseconds [9, 10]. A corona discharge is the segment of an electric discharge before the onset of a low-voltage, high-current arc, and essentially creates plasma in the transient or formative stage [10].

Traditional CDSI systems ignite a combustion process by initiating the thermal decomposition of fuel into radicals [11]. If the production of the radicals is produced by alternative means and in greater concentrations, the initial combustion rate can be accelerated [12]. TPI may accomplish this because the electron energy distribution function more closely matches the energy required to disassociate and ionize large hydrocarbon chain molecules [9]. As depicted in Figure 12, within 50 to 100 ns, TPI delivers pulses of 70 to 100 kV at currents from 450 to 600 A [13].   However, the total energy input is less than one Joule, and is comparable to capacitive discharge systems.

Furthermore, rather than a single intense arc, as in CD ignition, TPI distributes the ignition energy evenly among hundreds of streamers, filling a "cylinder" around the TPI electrode. Therefore, the ignition volume is four orders of magnitude larger and energetic radicals can be directly generated by TPI within this volume. Thus, the hypothesis is that TPI can generate multiple turbulent flames more rapidly, which will lead to shorter DDT times and distances [12].
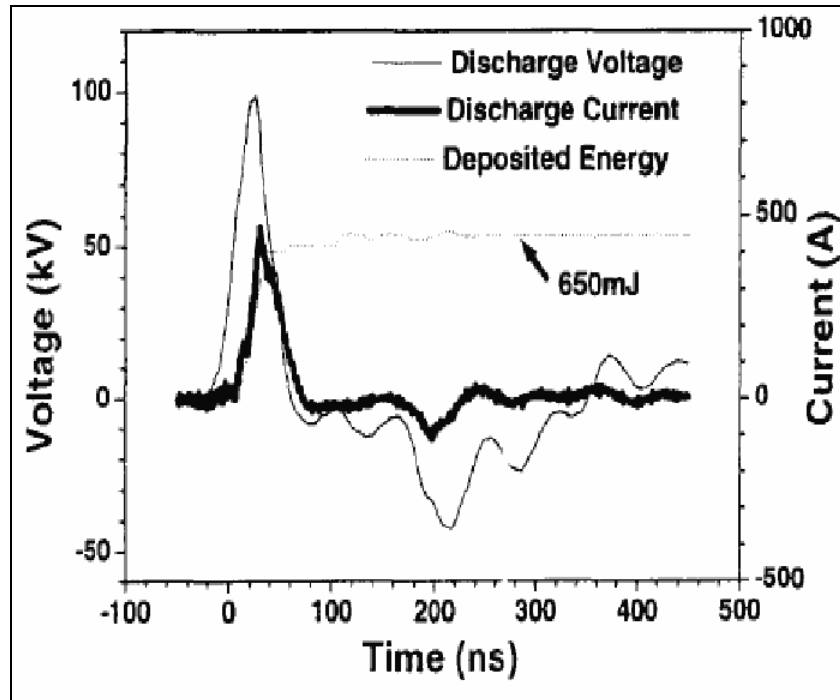

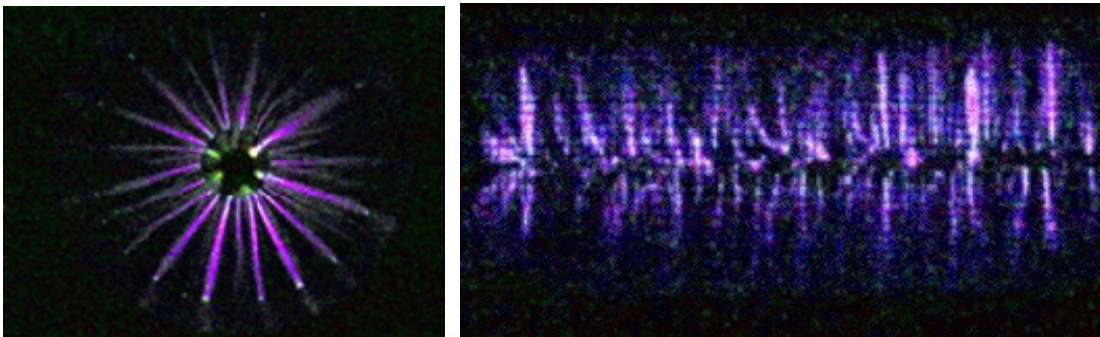Figure 12.   Typical Voltage, Current and Energy of TPI System (From Ref. 13)

Figure 13.   Axial and Radial Views of Corona Discharge (From Ref 14)

23

C.   COMBUSTOR INLET FLOW-CONDITIONING SCREENS

The use of flow conditioning screens at the combustor inlet was also explored. The motivation behind this approach was to improve the fuel-air mixing prior to entering the combustor while generating streamwise flow at the head end. Three different plates were designed with varying hole diameters (1/4 inch, 3/16 inch, and 1/8 inch) while keeping the porosity of the screen nearly constant. Depicted in Figure 14 are two of the screens: the 3/16 inch screen (left) and the 1/4 inch screen (right). The fuel/air mixture flowed through the annular pattern of holes while the larger center hole accommodated the TPI electrode.
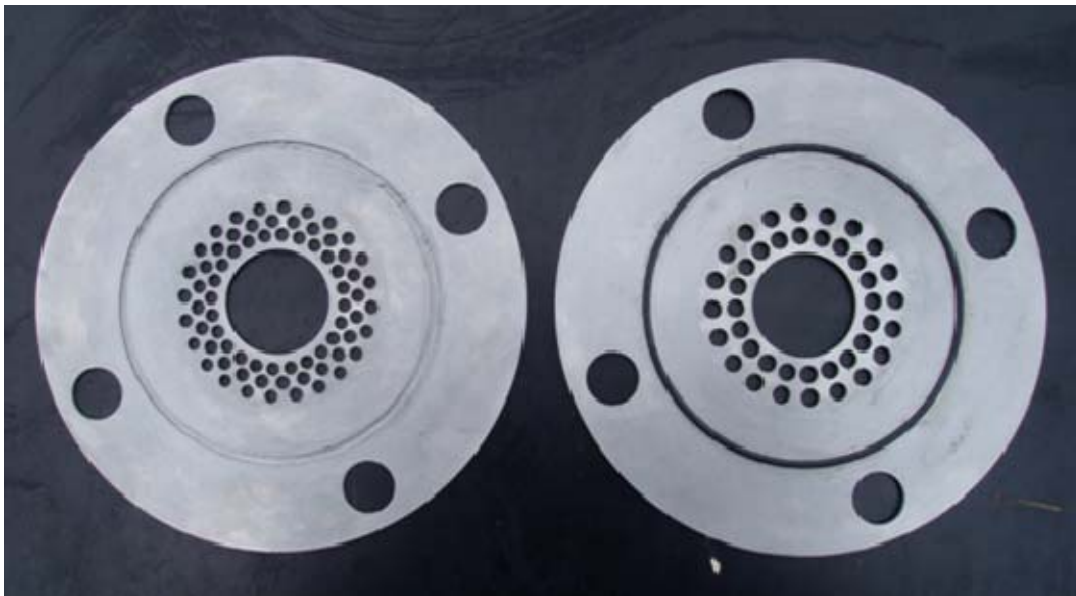

Figure 14.   Flow Conditioning Screens

IV.   EXPERIMENTAL SETUP

The experimental research for this thesis was conducted at the Naval Postgraduate School Rocket Propulsion Laboratory, Test Cell #1. The PDE was operated with gaseous ethylene and air for its fuel and oxidizer. Prior to conducting any testing, the test cell was completely rewired for test cell control and data acquisition. Further, the gas supply plumbing was modified to accommodate the reinstallation of the vitiator and a modified PDE. The following paragraphs provide a description of the hardware and software used in this effort.

A.   PDE
1. Combustion Tube

The PDE was based upon the combustion tube used in previous thesis work, including that of LT Joel Rodriguez [15]. The combustion tube itself was 3 in (7.62 cm) in diameter and 38 in (96.5 cm) long. It incorporated a sectional design to facilitate the placement and removal of turbulence generating devices. Six ports were tapped along the top of the tube to accommodate high-speed Kistler pressure transducers. Combustion pressures were the primary measurement for the determination of detonation and were used to calculate detonation wave speed, ignition delay time, and DDT distance. Two ports were also placed in the side of the tube for temperature measurements at the head and aft ends of the tube to monitor combustor conditions. A spiral was inserted in the combustor to help generate turbulence and accelerate the DDT process. The spiral was 30 in (76.2 cm) long and closely matched the internal diameter of the combustor.

2. Air and Fuel Delivery

The air and fuel delivery systems of the PDE were reengineered to achieve high frequency operation. This included modification of the air and fuel plumbing as well as the manifold of the PDE to accommodate a maximum of 0.40 kg/sec of total mass flow entering the engine. The most practical means of accomplishing this was to split the existing air delivery system in Test Cell #1 into four smaller lines, which could then be fed into an annular manifold at the head end of the combustion tube. Prior to entering the manifold, each of the four air delivery lines was coupled with a fuel line. High frequency

Valvetech solenoid valves delivered the fuel on demand such that a fuel/air mixture would enter the manifold from four lines at the beginning of each PDE cycle.
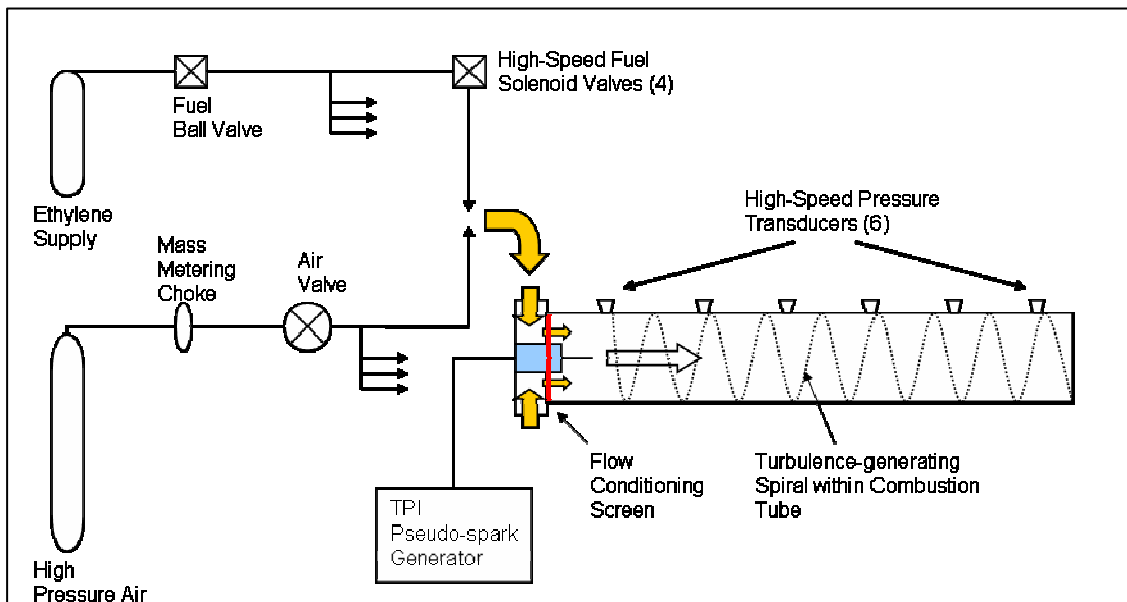

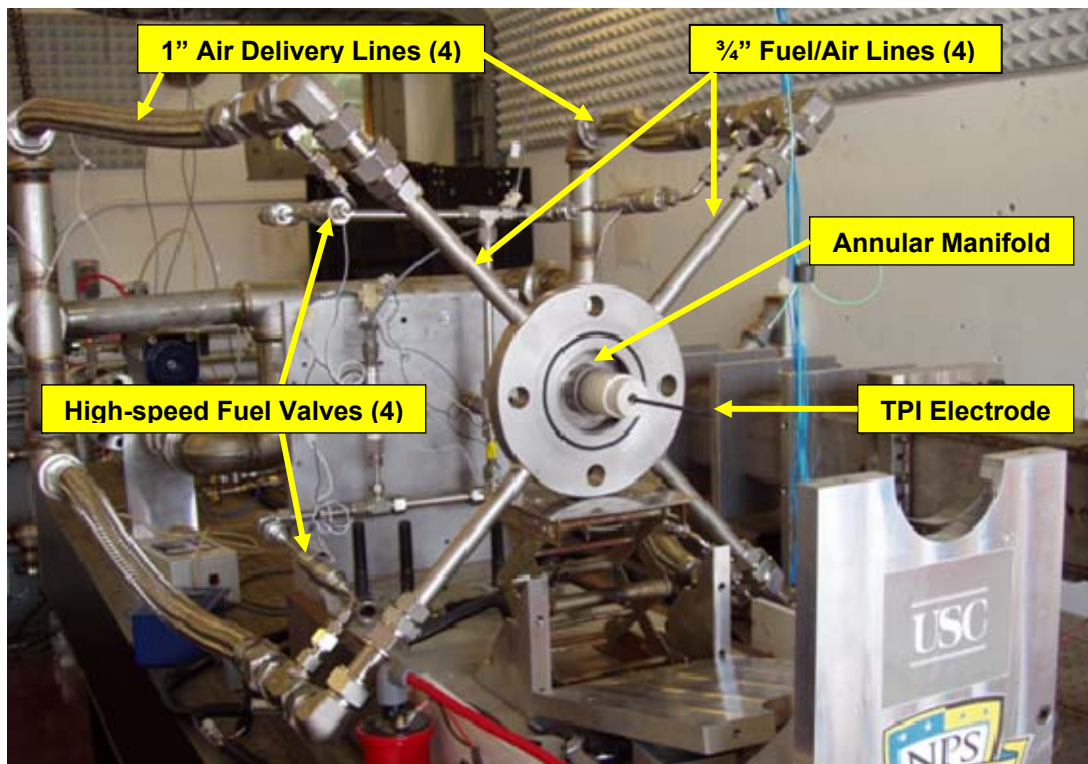
Figure 15.   PDE Schematic

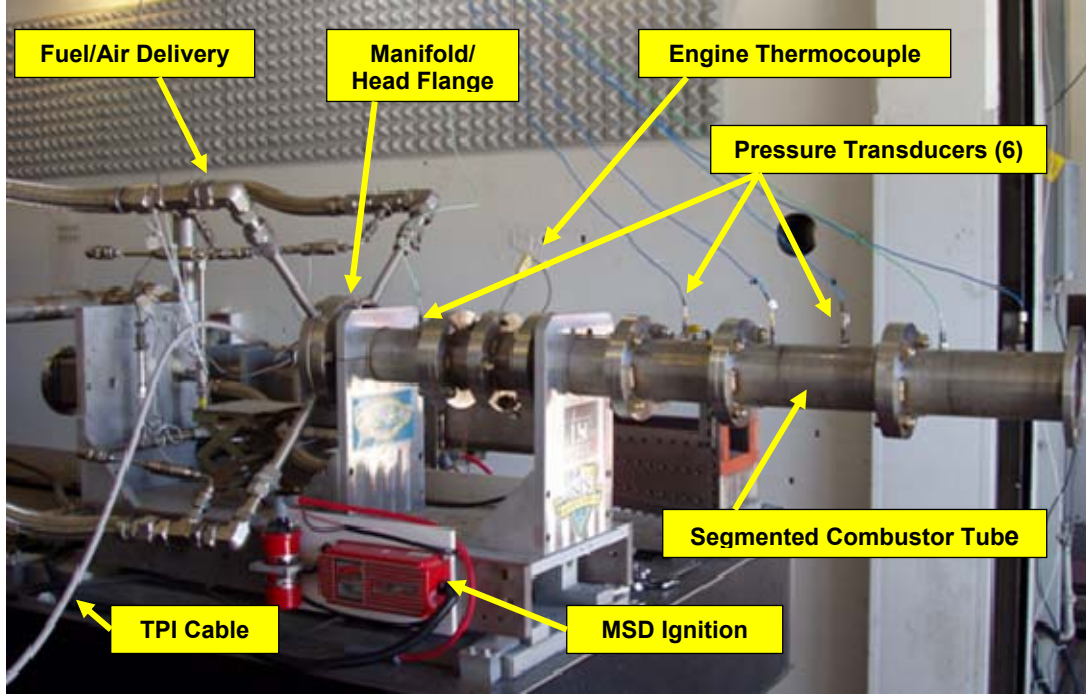

Figure 16.   PDE Fuel/Air Delivery

Figure 17. PDE

The total mass flow rate of air and fuel delivered to the engine was dependent upon the desired operation frequency, as explained in Section IIB. Individually, the mass flow rates of air and fuel were determined by the required equivalence ratio (φ). The equivalence ratio is a measure of a mixture's fuel/oxidizer ratio as compared to the stoichiometric ratio for that mixture, as defined by Equation (22):

$$\phi = \frac{\dot{m}_f / \dot{m}_o}{\left[\dot{m}_f / \dot{m}_o\right]_{stoichiometric}} \qquad (22)$$

A stoichiometric mixture ratio is one which does not leave any excess fuel or oxidizer after its chemical reaction. Thus, $\varphi > 1$ indicates the mixture was fuel rich, while $\varphi < 1$ signifies it was fuel-lean. For ethylene (C_2H_4) and air ($O_2 + 3.76N_2$), the stoichiometric chemical equation is represented by Equation (23):

$$C_2H_4 + 3(O_2 + 3.76N_2) \rightarrow 2CO_2 + 2H_2O + 3(3.76N_2) \qquad (23)$$
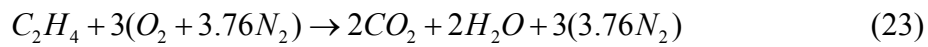
The stoichiometric mass ratio for ethylene/air is found by substituting the molecular weights into Equation (23), resulting in 6.799%.

With the stoichiometric ratio known, the required ratio could be determined for any given equivalence ratio by using Equation (22). Finally, the individual mass flow rates were calculated by taking the appropriate fractions of the total desired mass flow rate, as follows:

$$\dot{m}_{air} = \frac{\dot{m}_{total}}{\left[\dot{m}_f \middle/ \dot{m}_{air} \right]_{required} + 1} \qquad \text{and} \qquad \dot{m}_f = \dot{m}_{total} - \dot{m}_{air} \qquad (24)$$

High pressure air was supplied by four 3000 psig air tanks, regulated to a desired pressure, and entered Test Cell #1 via a single 2 inch stainless steel pipe. The mass flow rate of air was then established by regulating the air pressure upstream of a 0.236 inch choked orifice. The pressure required by the regulator for a specified mass flow rate could then be determined by the compressible, isentropic flow relationship below [16]:

$$\dot{m} = \left(\frac{A_2 p_t}{\sqrt{T_t}} \right) \Gamma_2 K_\Gamma \qquad (25)$$

$$\text{where} \quad K_\Gamma = \left[\left(\frac{g_c}{R} \right) \left(\frac{2\gamma}{\gamma-1} \right) \left(\frac{2}{\gamma+1} \right)^{2/(\gamma-1)} \left(\frac{\gamma-1}{\gamma+1} \right) \right]^{1/2} \qquad (26)$$

and $\Gamma_2 = 1$ (for choked flow).

The fuel supply lines did not require chokes. The mass flow rate of fuel was determined by regulating the upstream pressure which was set according to calibration plots of the Valvetech fuel valves. The valves were factory-calibrated to deliver specific mass flow rates at different supply pressures.

3. Ignition System

Three different ignition systems were compared in this effort. The first system was the TPI, as previously explained. Secondly, a high-performance automotive MSD capacitive discharge ignition system was used with a conventional Champion spark plug. The third system was a Unison capacitive discharge system with an aviation-grade spark plug. The Unison system allowed the total energy to be varied such that it could be compared with both the MSD system and TPI systems at their equivalent energy levels. During testing of all three systems, the timing of the ignition trigger with the fuel valve

sequence was adjusted to find the optimal timing conditions for that particular ignition system.

B.   VITIATOR

To simulate combustor stagnation conditions at different flight conditions, including supersonic cruise velocities, a vitiator was incorporated to heat the air entering the PDE. As a small combustor placed in the main air delivery line, the vitiator burned a hydrogen/air mixture to generate heat. Oxygen was then injected into the air delivery system downstream of the vitiator to restore the oxygen that was burned in the vitiator, correcting the molar concentration of oxygen to that of normal air. A hydrogen/air torch ignited the vitiator, and the operating temperature of the vitiator was varied to deliver air to the combustion chamber at up to 315°F.

Operating the PDE in this condition required a redesign of the mount for the TPI electrode. Previously, this device was fabricated out of nylon, as earlier thesis work with the TPI system did not employ vitiated air. Therefore, a new mount was required that could withstand the high temperatures while having the dielectric properties of nylon. Two suitable ceramic materials were chosen: Macor and Pyrolytic Boron Nitride (PBN). Identical electrode mounts were machined out of each ceramic to test their suitability in PDE applications.   Several factors constrained the design of the electrode mount, including the physical dimensions of the ceramic cylinders that were commercially and economically available.   Further, the mount was designed to accommodate the TPI system without any electrode alterations as well as fit into the head flange of the PDE with minimal modifications. The installation of a ceramic electrode mount in the head flange of the PDE is shown in the figure below.
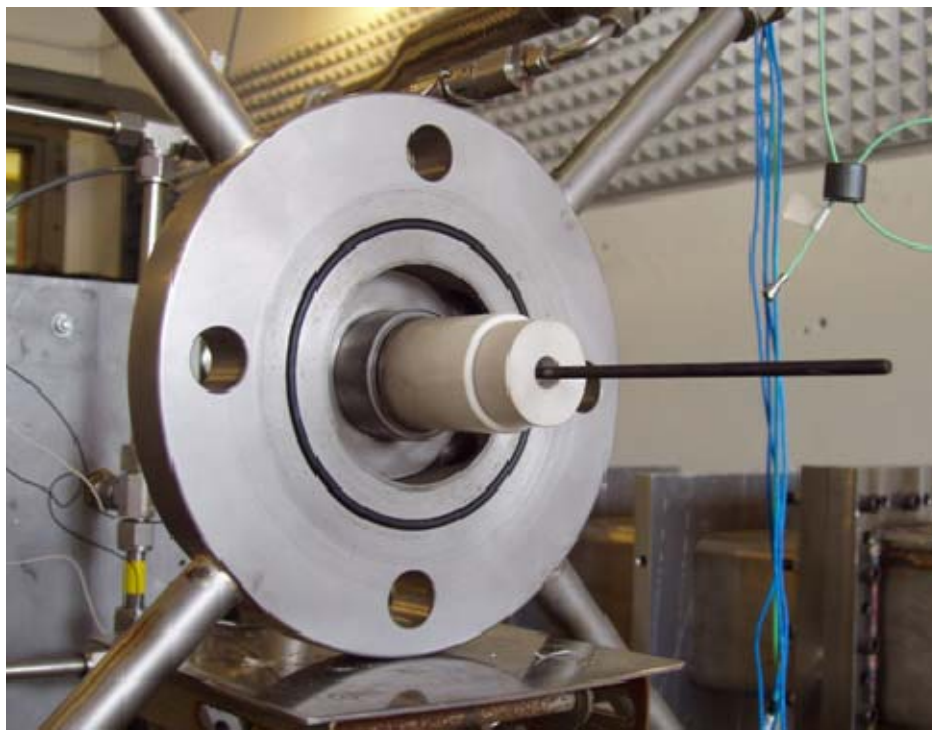
Figure 18.   Installation of TPI Electrode with Ceramic Mount

C.   FACILITY AND PDE CONTROL

Control of the test cell and PDE was accomplished primarily via a PC running National Instruments (NI) Labview 7.1, which was directly linked to a NI PXI-1000B controller inside the test cell. Additionally, within the control room was a Berkeley Nucleonics (BNC) Pulse Generator to send fuel valve and ignition trigger signals, switches for 28 VDC and 110 VAC power, and a safety switch with the capacity to shutdown the test cell in the event of an emergency. Regulator control software for the ER3000 controllers, operating on a separate PC, was utilized to control gas supply regulators and deliver the required pressures of all supply gases.

Both 28 VDC and 110 VAC were routed into the test cell on "switched" and "unswitched" power buses. The switched power required the facility to be enabled by the Labview software as well as resetting the emergency stop button. All ball valves and solenoid valves required switched power and would immediately close if the facility was disabled through software or if the emergency stop button was manually depressed. The unswitched power was used principally for instrumentation such that pressure transducers

and temperatures could always be monitored. A schematic diagram of the facility control and the Labview graphical user interface are presented in the figures below, while the wiring tables and test cell operating procedures are included in Appendices A and B.
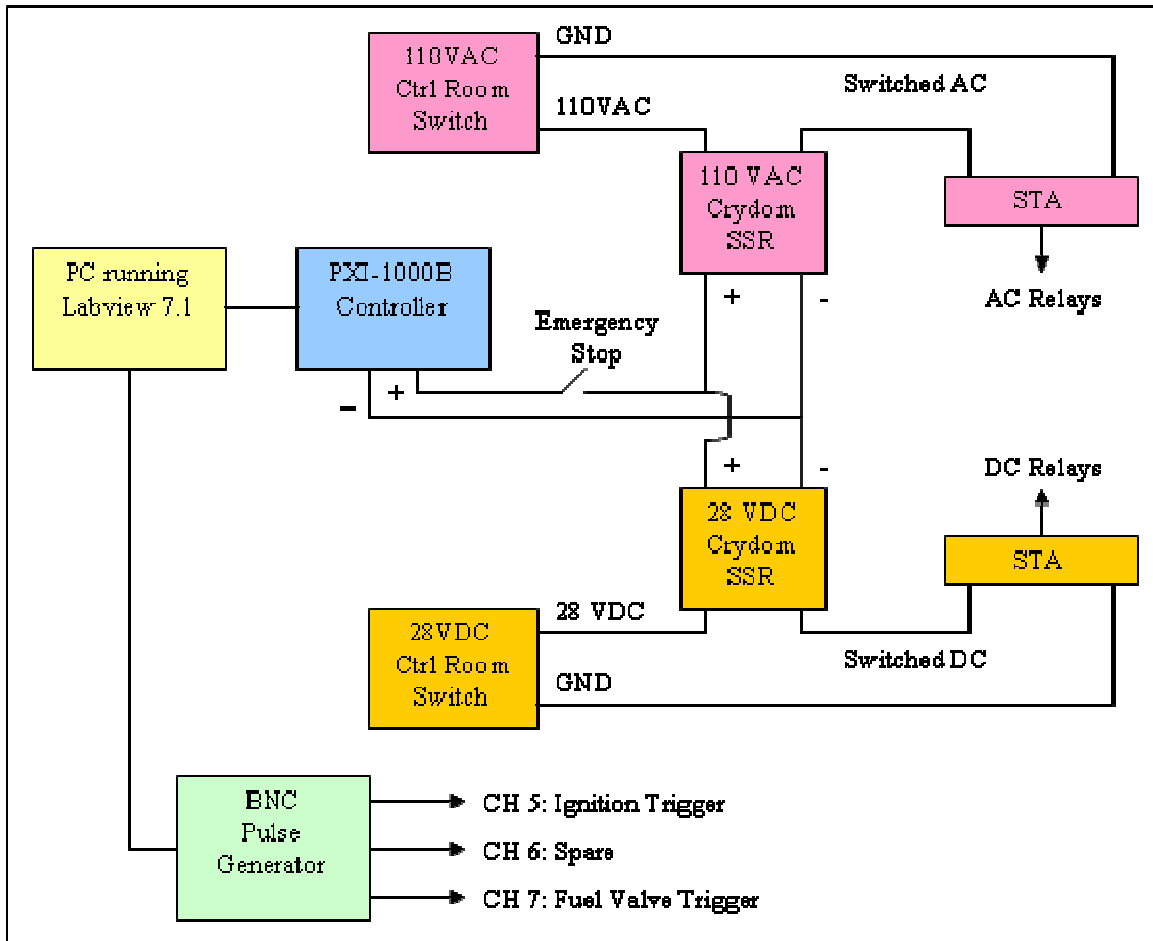

Figure 19.   Facility Control Schematic
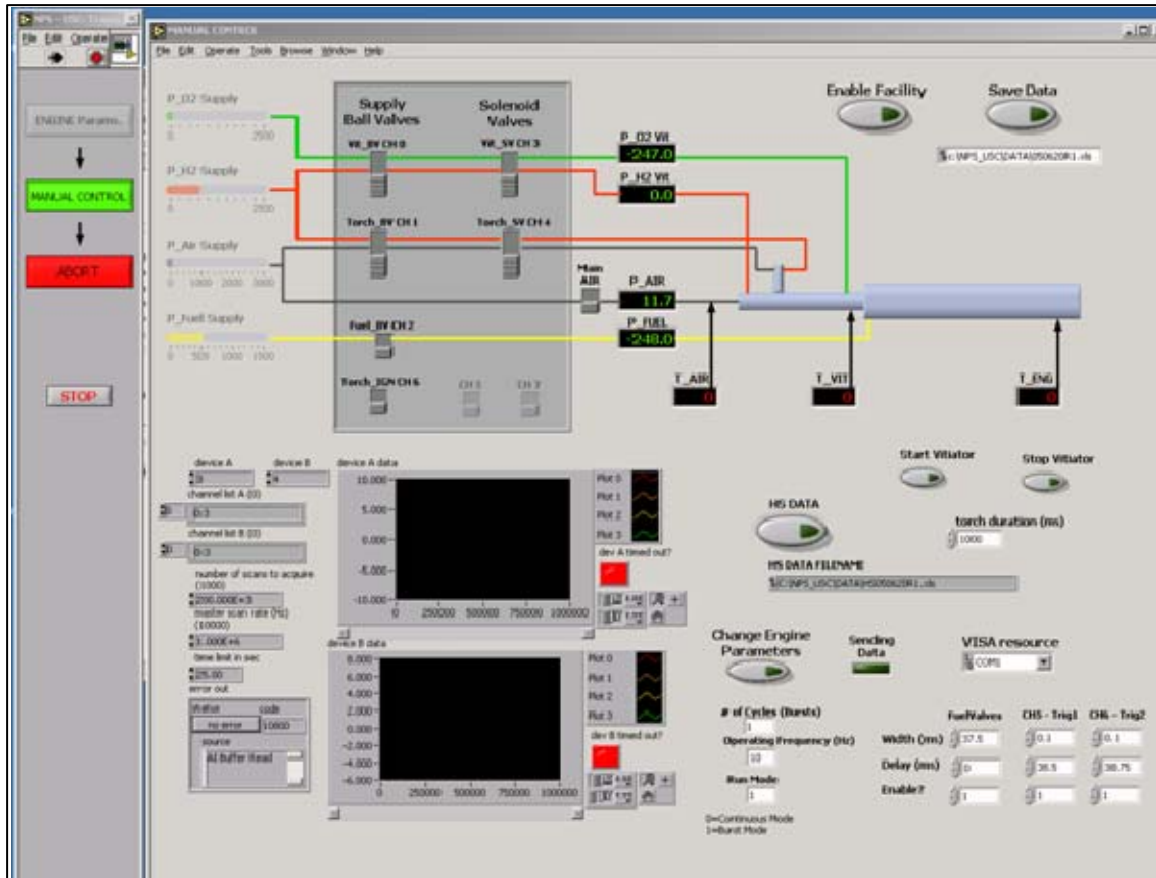
Figure 20.   Test Cell #1 GUI

D.   DATA ACQUISITION

Data acquisition was also accomplished by the control PC which was linked to the PXI-1000B. Four individual NI PXI-6115 cards were installed in the PXI-1000B with NI TB2705 interconnects, which could each monitor four instruments. Two cards were dedicated to acquire low-speed data, which included the temperature at the main air choke, the temperature at the entrance to the engine combustor, and the line pressures of the supply gases. The two remaining cards obtained high-speed data, which was comprised of the six Kistler high-speed pressure transducers, fuel pressure delivered to the high-frequency valves, and a record of the fuel valve trigger. Tables of the data acquisition and TB2705 wiring are included in Appendix A.

V.   RESULTS

The majority of the data in this work was obtained while operating the engine at 10 Hz in order to clearly remove shot-to-shot interference. At that rate, 10 cycles of data could be acquired for each engine run, while also providing for quick determination of successful ignition. Over 200 engine runs were completed in three separate testing campaigns, and the following paragraphs outline the results of this effort. It is important to note that in plotting the results, each data point is an average value of multiple samples of data in an effort to make true comparisons.

The figure below is an example of a pressure trace resulting from one combustion event in a 10 Hz run. The raw data was imported into Tecplot software to produce the pressure traces. The pressures registered by three of the six transducers are pictured. By dividing the known distance between two successive pressure transducers by the time between the initial pressure spikes recorded by those transducers, as measured on the pressure trace, the local wave speed could be calculated.
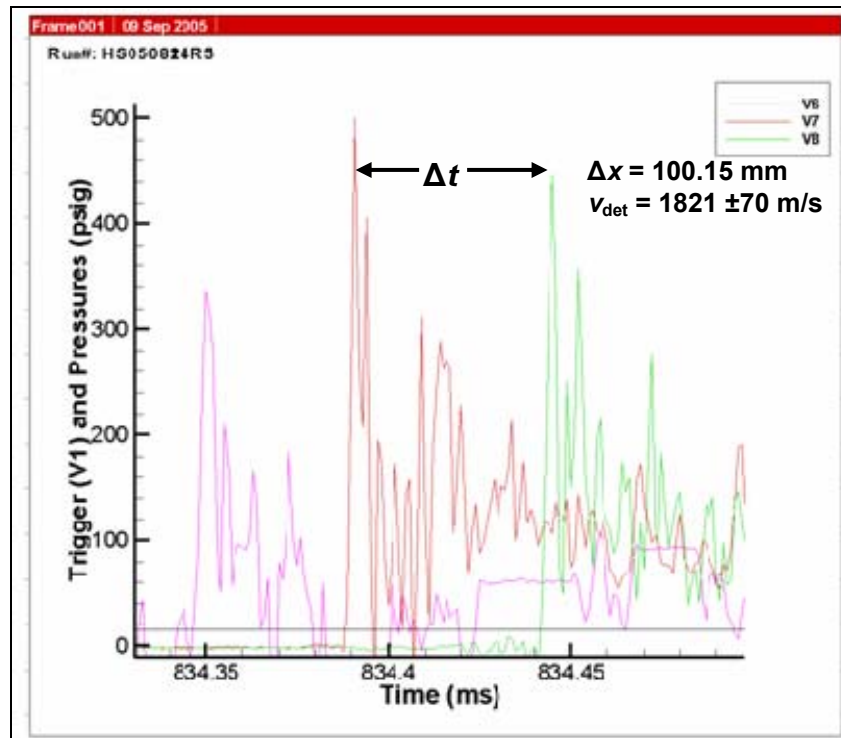

Figure 21.   Example of High Speed Pressure Data

A.   DETONATION SUCCESS RATE

The PDE was operated over a range of total mass flow rates, from 0.05 kg/s to 0.4 kg/s. Detonation success rates of the three ignition systems at the various mass flow rates are compared in Figure 22. Success rate is the foremost performance factor when deciding upon an ignition strategy for PDEs. The engine must detonate on every cycle for it to effectively generate thrust at higher frequencies. At the lowest mass flow rate, all three ignition systems could achieve detonation in ethylene/air mixtures over a range of equivalence ratios. However, the MSD capacitive discharge system began to fail at 0.1 kg/sec, and the Unison system behaved similarly at 0.15 kg/sec. At higher flow rates, the CD systems were extinguished before they could initiate combustion. However, TPI continued to achieve 100% detonation success up through 0.3 kg/sec. The performance began to deteriorate at 0.35 kg/sec.

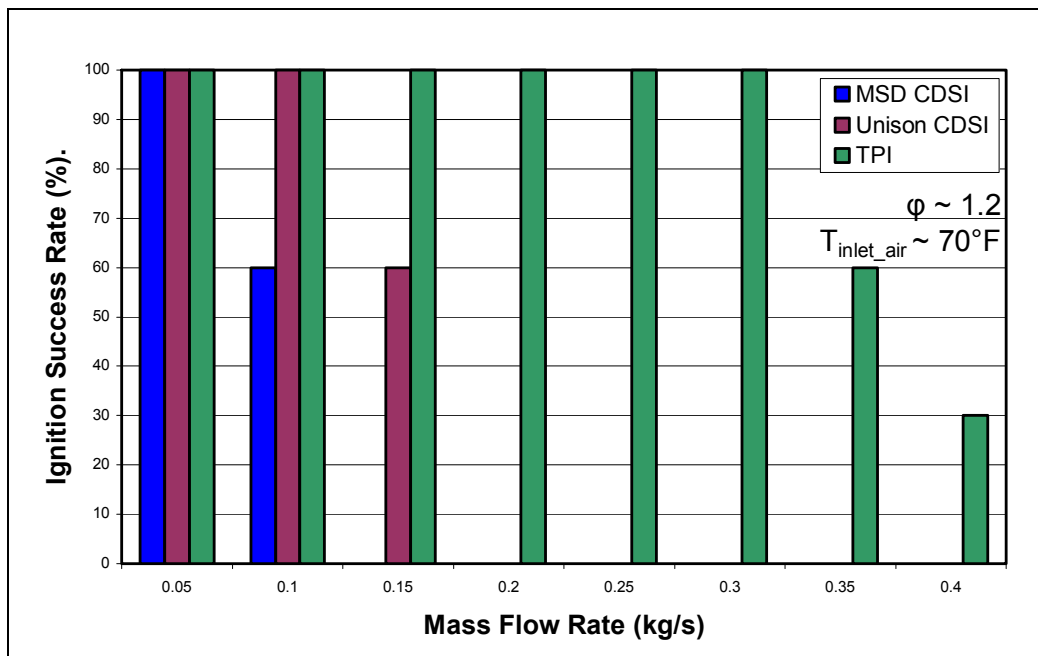Figure 22.   Ignition Success Rate vs. Mass Flow Rate

B.   IGNITION DELAY TIME

The second performance parameter examined was ignition delay time, as this measurement has direct correlation to DDT time. Ignition delay time was defined as the time from an electrical discharge to the time at which the pressure increased one atmosphere at the head end of the engine. Figure 23 compares the two capacitive

discharge systems at 0.05 kg/s, at which both systems could achieve 100% success rates. At this flow rate, the Unison system was set to deliver 70 mJ to compare it to the energy input of the MSD ignition system, and the Unison system achieved a noticeable improvement in ignition delay time, ranging from 0.6 ms to 1.3 ms. Due to an error in fuel pressure settings, the equivalence ratio in this particular comparison was higher than targeted, but the trend is still valid.

The equivalence ratio plotted in these results is the value calculated in post-run analysis. It was calculated by using the actual temperature and air pressure at the main air choke and the fuel pressure entering the high-speed fuel valves to determine the respective mass flow rates. However, previous work at the NPS RPL has shown that the high-speed fuel valves create variations in equivalence ratio along the length of the combustor tube, ranging from fuel-rich at the head-end to fuel-lean at the open-end [17]. For example, at a target equivalence ratio of 1.0, the true equivalence ratio as measured by optical spectroscopic diagnostics may vary from 1.2 at the head-end to 0.9 at the aft-end. Nevertheless, the equivalence ratio presented in these results was derived in a consistent manner as discussed above to offer true comparisons.
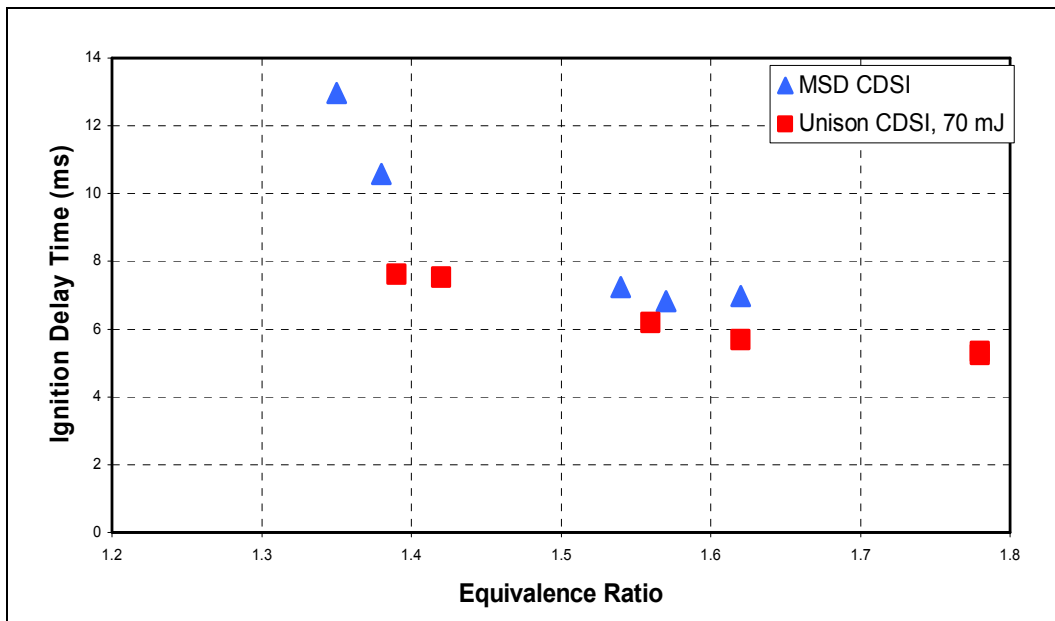

Figure 23.   Ignition Delay Time vs. Equivalence Ratio (Mass Flow Rate = 0.05 kg/s)

Figure 24 presents a comparison of all three ignition systems at 0.10 kg/s. At this higher flow rate, the MSD system did not achieve 100% success and its ignition delay time was excessive and wide-ranging. The Unison system was adjusted to deliver 1 J to more closely approximate the energy input of TPI. (At the previous setting of 70 mJ, the Unison system failed to achieve 100% success rates at 0.10 kg/s). At that setting, both systems performed equally in terms of ignition delay time.

The signal to trigger the Unison system had to be sent 19 ms before the fuel valves closed to allow for its charge /discharge time. This could prove to be excessive at higher operating frequencies as cycles would begin to overlap. The TPI trigger, however, was consistently sent 1 ms after the fuel valves closed, at which point it would charge and then discharge 185 μs later. This condensed and reliable time scale is essential for high frequencies.

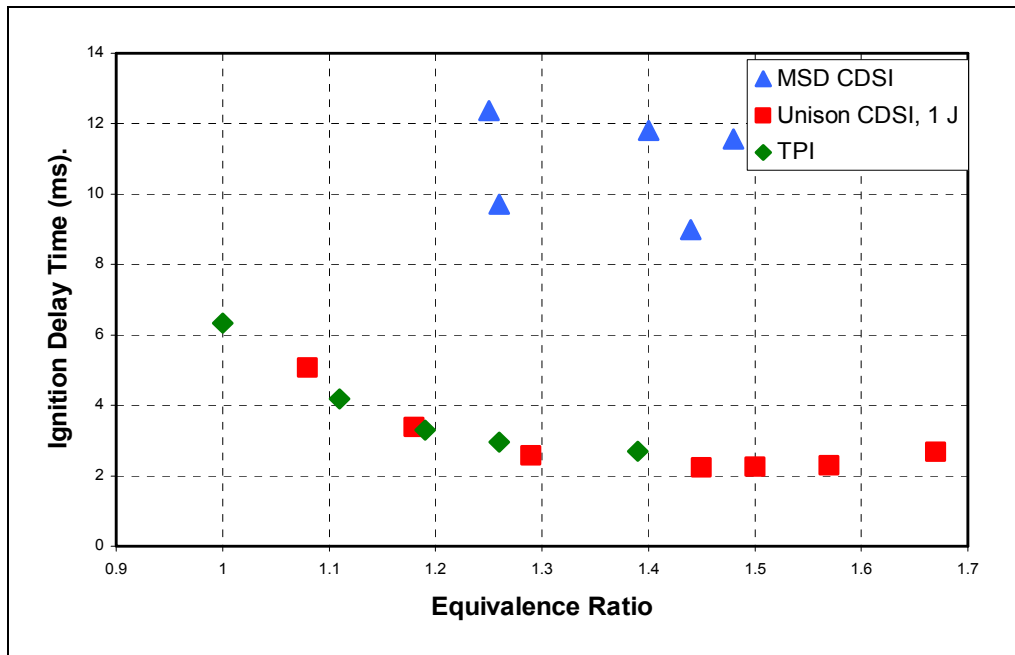Figure 24.   Ignition Delay Time vs. Equivalence Ratio (Mass Flow Rate = 0.1 kg/s)

The ignition delay time achieved by TPI at 0.20 kg/s is shown in Figure 25 along with the measured detonation wave speeds. TPI was the only ignition system that reliably achieved 100% ignition at the higher flow rate of 0.20 kg/s. Two testing campaigns were compared and provided consistent results for ignition delay time. At a

36

measured equivalence ratio of 1.27, the ignition delay time of TPI reached a minimum of 2.7 ms. Meanwhile, the detonation wave speed remained fairly constant at about 1.9 km/sec, appearing only slightly with higher with increasing equivalence ratio, which may have been due to locally overdriven conditions.

The effect of mass flow rate on ignition delay time was also studied. Figure 26 shows that the ignition delay time was not greatly influenced by mass flow rate, as it was relatively consistent at about 4.1 ms at an equivalence ratio of 1.03. Doubling the flow rate from 0.2 kg/s to 0.4 kg/s only increased the ignition delay time by 0.14 ms.
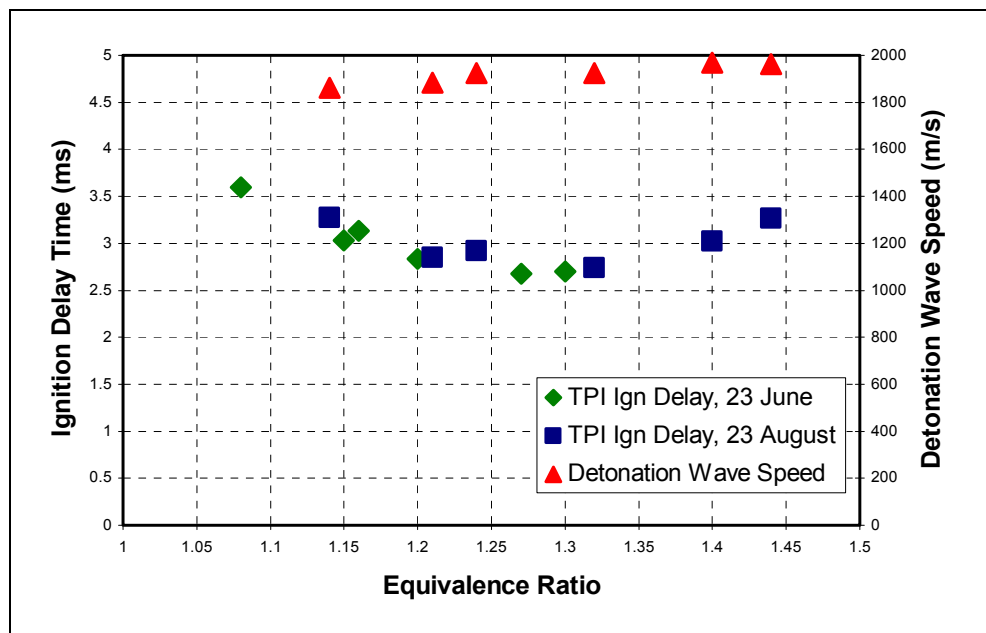

Figure 25.   TPI Ignition Delay Time and Detonation Wave Speed vs. Equivalence Ratio
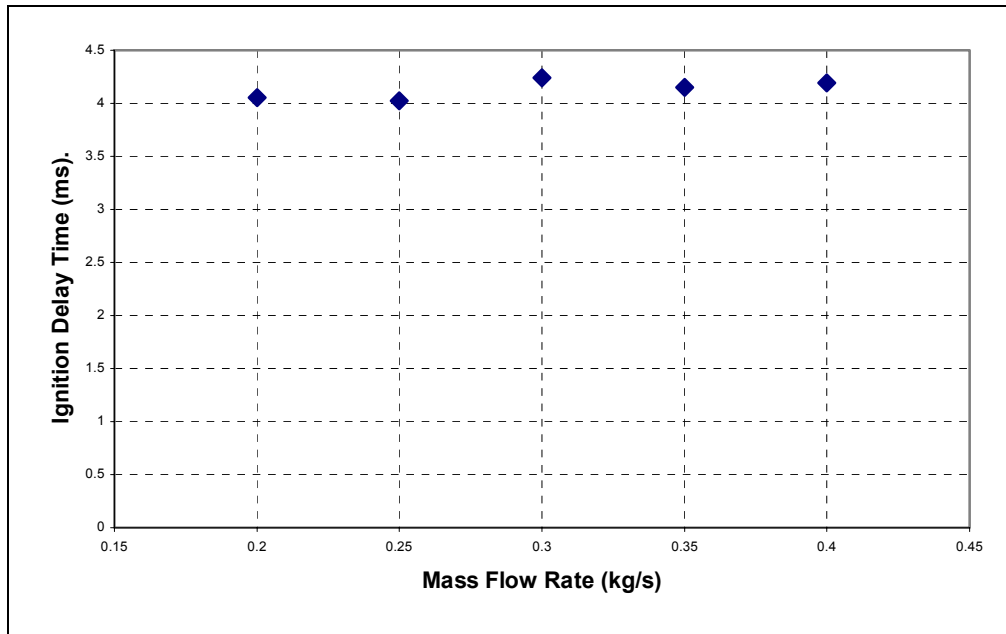(Mass Flow Rate = 0.20 kg/s)

Figure 26.   TPI Ignition Delay Time vs. Mass Flow Rate (φ ~ 1.03)

C.   EFFECTS OF FLOW CONDITIONING SCREENS

Inserting screens at the engine manifold produced mixed results. As shown in Figure 27, the ignition delay time was reduced by the addition of a screen at 0.20 kg/s, but the reduction did not exactly follow the hole size of the screens. The screen with larger ¼ inch holes generally resulted in shorter times than the screen with 3/16 inch holes. However, inserting the screen with 1/8 inch holes resulted in the shortest ignition delay times, reducing the average ignition delay time by 0.48 ms compared to operations with no screen.

It would appear that if only considering the results in Figure 27, using a screen would increase the initiation performance of a PDE. However, the addition of screens reduced the ignition success rates at higher mass flow rates, as shown in Figure 28. At 0.20 kg/s, the ignition success rate was 100%, but that rate could not be maintained at 0.3 kg/s for the ¼ inch screen or even 0.25 kg/s for the smaller meshes. It appears that the ignition event is also dependent upon some recirculation at the head-end which the screens may have eliminated by effectively aligning the flow. Further examination of the effects of adding screens is required, including turbulence measurements of the head-end

38

flow. Though, there appears to be some promise in the reduction of ignition delay time if the reasons for ignition failure can be determined.
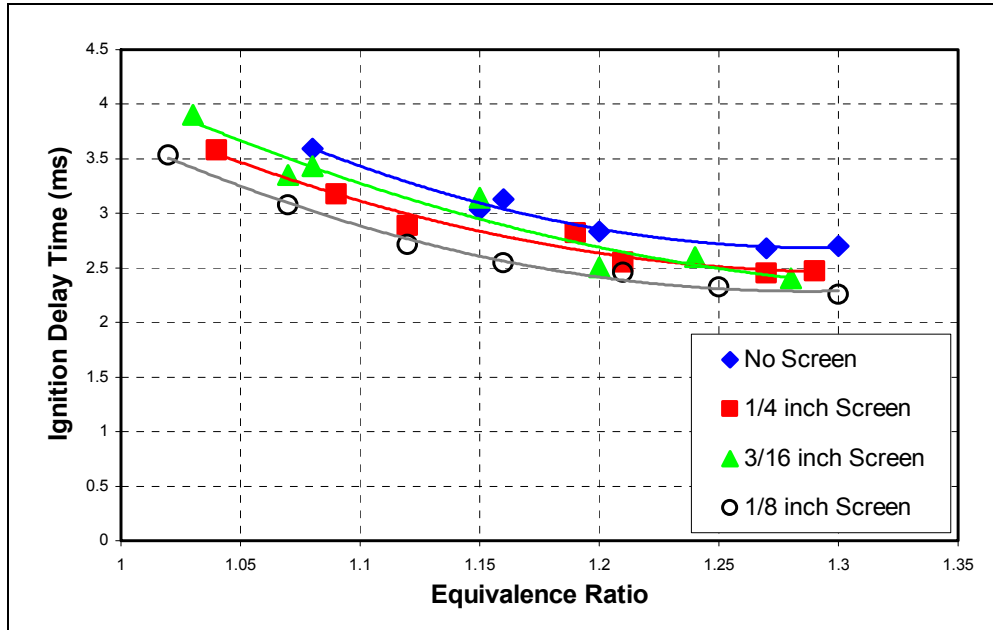
Figure 27.   Screen Comparison: TPI Ignition Delay Time vs. Equivalence Ratio (0.20 kg/s)
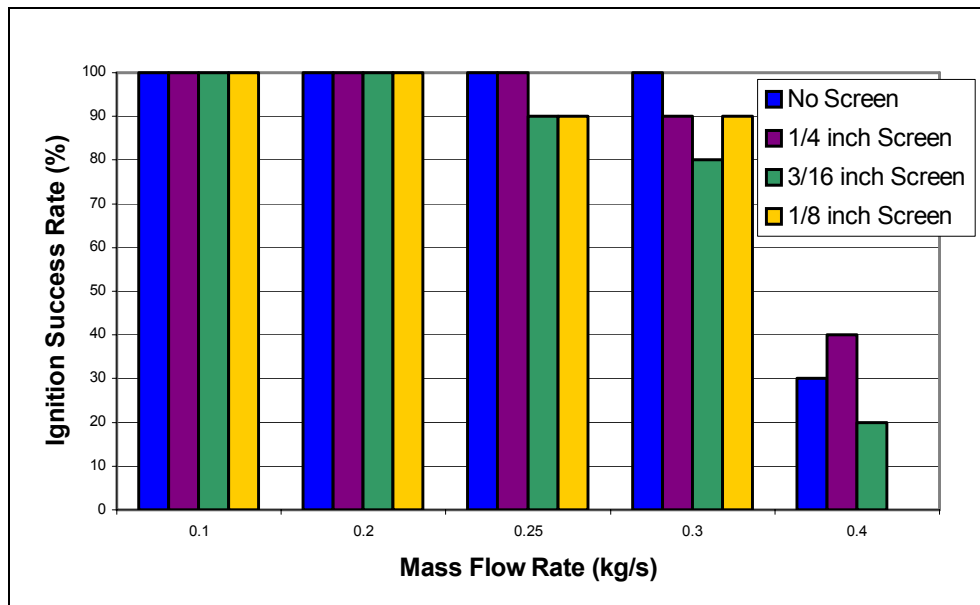
Figure 28.   Screen Comparison: Detonation Success Rate vs. Mass Flow Rate

D. PERFORMANCE WITH VITIATED AIR

Figure 29 compares the results of operating the PDE with reactants at increased temperatures entering the combustion chamber. The temperature conditions were chosen to represent realistic stagnation temperatures within a combustion chamber at various flight conditions, including 315°F at Mach 2.16 cruise. As the temperature was increased, ignition delay time steadily declined. The lowest average ignition delay time of the study was achieved when the temperature of the reactants was 315°F, resulting in 1.7 ms. Meanwhile, the temperature did not have an apparent effect on detonation velocity, as it remained within 35 m/s of the average 1.86 km/s. Therefore, the benefits of TPI previously discussed appear to improve with increasing flight Mach number.

Figure 29. Effect of Combustor Air Temperature (Mass Flow Rate = 0.20 kg/s, $\varphi \sim 1.24$)

VI.   CONCLUSIONS AND FUTURE WORK

The Unison capacitive discharge system had comparable ignition delay time to TPI at the lower flow rate of 0.10 kg/s. They both achieved marked improvement over the MSD system, which could only produce 100% ignition rates at the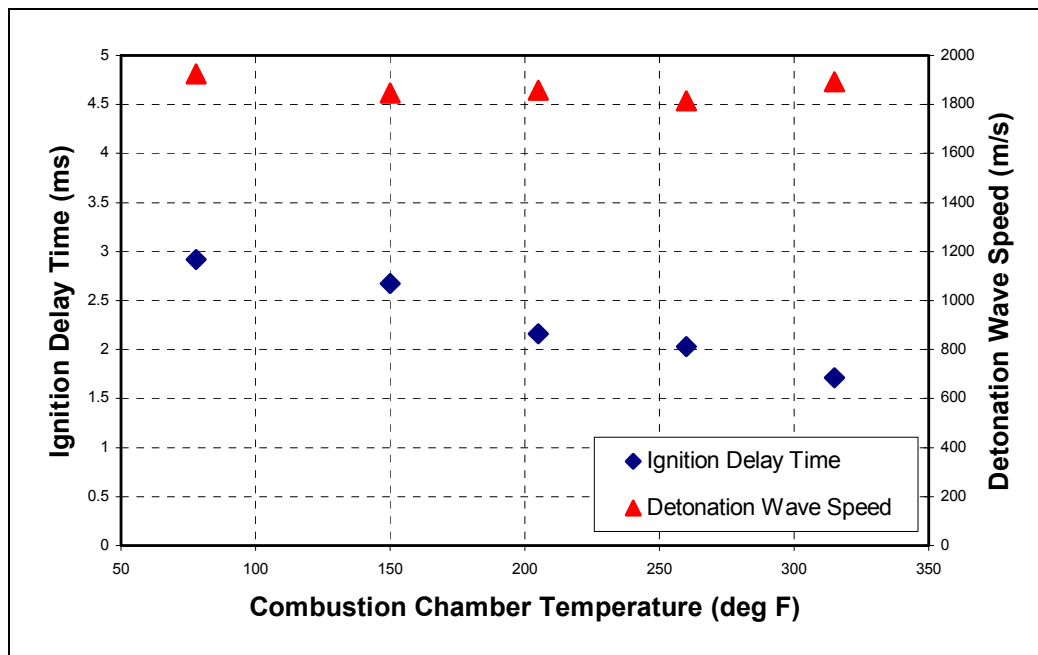 lowest mass flow rate. At mass flow rates in excess of 0.10 kg/s, however, only TPI provided consistent ignition. The higher flow rates are required for practical systems to result in realistic Mach fill rates approaching 0.2. The TPI system provided reliable performance at up to 0.3 kg/s, which corresponded to a fill Mach number of 0.163. Further, the consistent timing and rapid charge rate of TPI is essential for high frequency operations.

Inserting a screen at the head-end of the engine appears to hold promise for further reduction in DDT time. Further study is required to characterize the turbulent flow in the combustion chamber and determine why the screens prevented reliable ignition at higher flow rates.

Operating the PDE with vitiated air validated the study with realistic combustion chamber inlet temperatures of a supersonic flight vehicle. The TPI system provided consistent ignition and reduced ignition delay times which continued to decrease with increasing temperature.

Finally, using TPI, the PDE was operated at detonation frequencies up to 40 Hertz, which was a milestone achievement for a PDE without supplementary oxygen at the NPS RPL. Future PDE development at the RPL will eliminate the fuel/oxygen initiator, as this effort has proven that auxiliary oxygen is not required, thus increasing the fuel-based specific impulse of future designs.

Operating frequencies in excess of 40 Hz may be accomplished by redesigning the air flow through the head end of the current PDE. Reliable operation of the engine was limited to flow rates of 0.3 kg/s due to the air velocity around the ignition system, and was not due to limitations of TPI. Achieving higher mass flow rates, and thus higher frequencies, will be possible with a design that reduces the flow velocity past the electrode.

THIS PAGE INTENTIONALLY LEFT BLANK

APPENDIX A: WIRING TABLES

AC Relays:

Relay Number	Logic Input	Controls:
AC 1/0	DIO 0	Vitiator (O_2/H_2) Ball Valves
AC 1/1	DIO 1	Torch (H_2/Air) Ball Valves
AC 1/2	DIO 2	Fuel Ball Valve
AC 1/3	DIO 3	Vitiator (O_2/H_2) Solenoid Valves
AC 2/0	DIO 4	Torch (H_2/Air) Solenoid Valves
AC 2/1	DIO 5	Spare
AC 2/2	DIO 6	Torch Ignition
AC 2/3	Enable Signal	Main Air Ball Valve (Air Isolation Valve)

DC Relays:

Relay Number	Logic Input	Controls:
DC 0/0		Spare
DC 0/1	BNC CH 7	High Speed Fuel Valves (1&2)
DC 0/2	BNC CH 7	High Speed Fuel Valve (3)
DC 0/3	BNC CH 7	High Speed Fuel Valve (4)

Table 4.   Electrical Relay Assignments

Low Speed Data

Channel	Data
Device 1 ACH 0	Main Air Choke Temperature
ACH 1	Engine Temperature
ACH 2	Main Air Choke Pressure
ACH 3	Fuel Pressure
Device 2 ACH 0	Hydrogen Pressure
ACH 1	HP Air Pressure (Torch Air)
ACH 2	Oxygen Pressure
ACH 3	Spare

High Speed Data

Channel	Data
Device 3 ACH 0	Record Fuel Valve Trigger
ACH 1	Fuel Pressure
ACH 2	Kistler High Speed Pressure 1
ACH 3	Kistler High Speed Pressure 2
Device 4 ACH 0	Kistler High Speed Pressure 3
ACH 1	Kistler High Speed Pressure 4
ACH 2	Kistler High Speed Pressure 5
ACH 3	Kistler High Speed Pressure 6

Table 5.   Data Acquisition Assignments

Device #	Pin Label	Destination	Wire Color	Pin #
1	DAC0 OUT	Facility Enable +	R	22
1	AO GND	Facility Enable -	W/B	54
1	DAC1 OUT	Spare +	G	21
1	AO GND	Spare -	W/B	54
1	DIO 0	MS4 AC Relay 1/0 Logic	R	52
1	DIO 1	MS4 AC Relay 1/1 Logic	B	17
1	DIO 2	MS4 AC Relay 1/2 Logic	G	49
1	DIO 3	MS4 AC Relay 1/3 Logic	W	47
1	DIO 4	MS4 AC Relay 2/0 Logic	R	19
1	DIO 5	MS4 AC Relay 2/1 Logic	B	51
1	DIO 6	MS4 AC Relay 2/2 Logic	G	16
1	DIO 7	Open	W	48
1	+5V OUT	+5V MS4 Relays	R	8
1	DGND	GND MS4 Relays	B	18
1,2,3,4	ACH0+		R	68
1,2,3,4	ACH0-		B	34
1,2,3,4	ACH1+	Low-Speed/High-Speed Data Acquisition (See Data Acquisition Tables)	G	33
1,2,3,4	ACH1-		W	66
1,2,3,4	ACH2+		R	65
1,2,3,4	ACH2-		B	31
1,2,3,4	ACH3+		G	30
1,2,3,4	ACH3-		W	63

Table 6.   NI TB2705 Pin Assignments

APPENDIX B: TEST CELL #1 SOP

Test Cell #1
Standard Operating Procedures (SOP)
(last modification date 15 AUG 05)

Prior to starting preparations
1. Notify all lab personnel of live test cell.
2. Turn ON warning lights
3. Notify the Golf Course (x2167) (Only required if Hot Fire Test is conducted)

Preparing Test Cell
In Control Room
1. Push Emergency Stop Button IN (secured) prior to entering test cell
2. Turn Center Console power ON
3. Turn BNC power ON (Cabinet #2)
4. Turn 24 VDC and 110 VAC ON (Cabinet #1A)
5. Boot up SCARP

Outside
1. Turn ER3000/Tescom power ON (Switch in Test Cell 2)
2. Attach combustion tube
3. Attach Kistlers and thermocouple (Ensure Kistler Amps are OFF)
4. Turn Kistler Amps ON (Single switch on power strip)
   a. Set MU/V to desired gains
   b. Set to OPERATE
5. Shop Air Valve OPEN (Valve on table and check red handle)
6. Main Air Ball Valve OPEN (diverting air to Test Cell 1)
7. Main Air OPEN (Blue Jamesbury HP Air Tank Valve)
   NOTE: Valve should be opened slowly as not to shock the lines
8. Supply Gas Bottles OPEN

TPI Equipment
1. Turn 3-phase AC power ON (Breaker 5, Panel C)
2. Oscilloscope ON
3. Pulse Generator ON
4. Waveform Generator ON
   NOTE: Should be 10 kHz, Burst Mode, Square Wave
5. Pseudospark Generator:
   a. Check Heater set to 0
   b. Breaker ON; (After ~ 30 seconds, should hear click)
   c. Heater ON; (Keep Alive not needed)
   d. Heater slowly to 30, wait 1 minute;
      Heater slowly to 60, wait 1 minute;
      Heater slowly to desired setting (75 to 80, maximum)

45

Test Cell #1
Standard Operating Procedures (SOP)

Securing Test Cell

1. Vent Fuel and Vitiator Gas Lines
2. Ensure Node 1, Node 3 are set to ZERO (& Nodes 2, 4, & 5 if vitiator used)
3. Ensure all BV have been CLOSED
4. Disable facility
5. Stop Control Code
6. Push Emergency Stop Button IN
7. Turn OFF 24 VDC and 110 VAC power supplies
8. Turn OFF BNC Power Supply

9. Secure Main Air (HP Air valve in Closed position)
10. Secure Supply Gases

TPI Equipment
1. On Pseudospark Pulse Generator:
   a. Heater knob to ZERO (normally set to 75-80)
   b. Heater switch to OFF (Down)
   c. Three-switch Breaker OFF (Listen for "click" from inside unit)
   d. Turn 3-phase AC power OFF (Breaker 5, Panel C)

Test Cell
1. Turn OFF power strip for Kistler Amps
2. Remove Kistler lines and Engine Thermocouple
3. Remove combustion tube
4. Close Main Air for Test Cell 1 (Light Blue Jamesbury)
5. Close Shop Air (Isolation valve on table)
6. Secure TESCOM power in Test Cell #2
7. Stow Cameras and other equipment used in testing.
8. Close Test Cell 1

9. Turn OFF Warning Lights.
10. Secure Central Console power

Test Cell #1
Standard Operating Procedures (SOP)

Running the Engine (COLD FLOW)

1. Set Engine Parameters (Send to BNC when area is <u>clear</u>)
2. Edit data save location for Low and High Speed Data
     a. Low speed: c:\NPS_USC\DATA\0508xxRxx.xls
     b. High speed: c:\ NPS_USC\DATA\HS0508xxRxx.xls
3. Enter amount of data required at 1e6 Hz
4. Set Fuel Pressure (Node 3) on ER3000
5. Preset Air Pressure (Node 1) on ER3000 (**but leave set at ZERO)**
     NOTE: Setting Air Pressure will start air flow.
6. Clear test cells/head count
7. Emergency Shutdown Button OUT (Test cell is now live)
8. In Labview, Enable Facility
9. Fuel Ball Valves OPEN

10. Verify Golf Course is clear, turn Siren ON
11. Press RECORD on VCR
12. Click SAVE DATA (Button turns green)
13. Select *preset* Air Pressure on Node 1 (Air starts flowing)
14. After Air Pressure rises, click HS DATA (button flashes green)
15. Press START on BNC
     WARNING: The engine will now fire

16. Select *zero* Air Pressure on Node 1
17. Siren OFF
18. Stop VCR
19. Click SAVE DATA (Green light goes out)
20. Fuel Ball Valves CLOSED
21. Disable facility
22. Push Emergency Stop Button IN

Test Cell #1
Standard Operating Procedures (SOP)

Running the Engine (VITIATED FLOW)

1. Set Engine Parameters (Send to BNC when area is <u>clear</u>)
2. Edit data save location for Low and High Speed Data
   a. Low speed: c:\NPS_USC\DATA\0508xxRxx.xls
   b. High speed: c:\ NPS_USC\DATA\HS0508xxRxx.xls
3. Enter amount of data required at 1e6 Hz
4. Set required pressures on ER3000:
   a. Oxygen (Node 2)
   b. Hydrogen (Node 5)
   c. Fuel (Node 3)
5. Preset Air Pressure (Node 1) on ER3000 (**but leave set at ZERO)**
   NOTE: Setting Air Pressure will start air flow.
6. Clear test cells/head count
7. Emergency Shutdown Button OUT (Test cell is now live)
8. In Labview, Enable Facility
9. Torch, Vitiator and Fuel Ball Valves OPEN

10. Verify Golf Course is clear, turn Siren ON
11. Press RECORD on VCR
12. Click SAVE DATA (Button turns green)
13. Select *preset* Air Pressure on Node 1 (Air starts flowing)
    NOTE: Then monitor Hydrogen (Node 5) to secure if necessary
14. After Air Pressure rises, click START VITIATOR
    NOTE: Check for rising Engine Temperature
15. At target Engine Temperature, click HS DATA (button flashes green)
16. Press START on BNC
    WARNING: The engine will now fire

17. Select *zero* Hydrogen Pressure on Node 5
18. Click STOP VITIATOR
19. AFTER Eng Temp decreases through 140°, select *zero* Air Pressure on Node 1
20. Siren OFF
21. Stop VCR
22. Click SAVE DATA (Green light goes out)
23. Torch, Vitiator, and Fuel Ball Valves CLOSED
24. Disable facility
25. Push Emergency Stop Button IN

APPENDIX C: ENGINEERING DRAWINGS

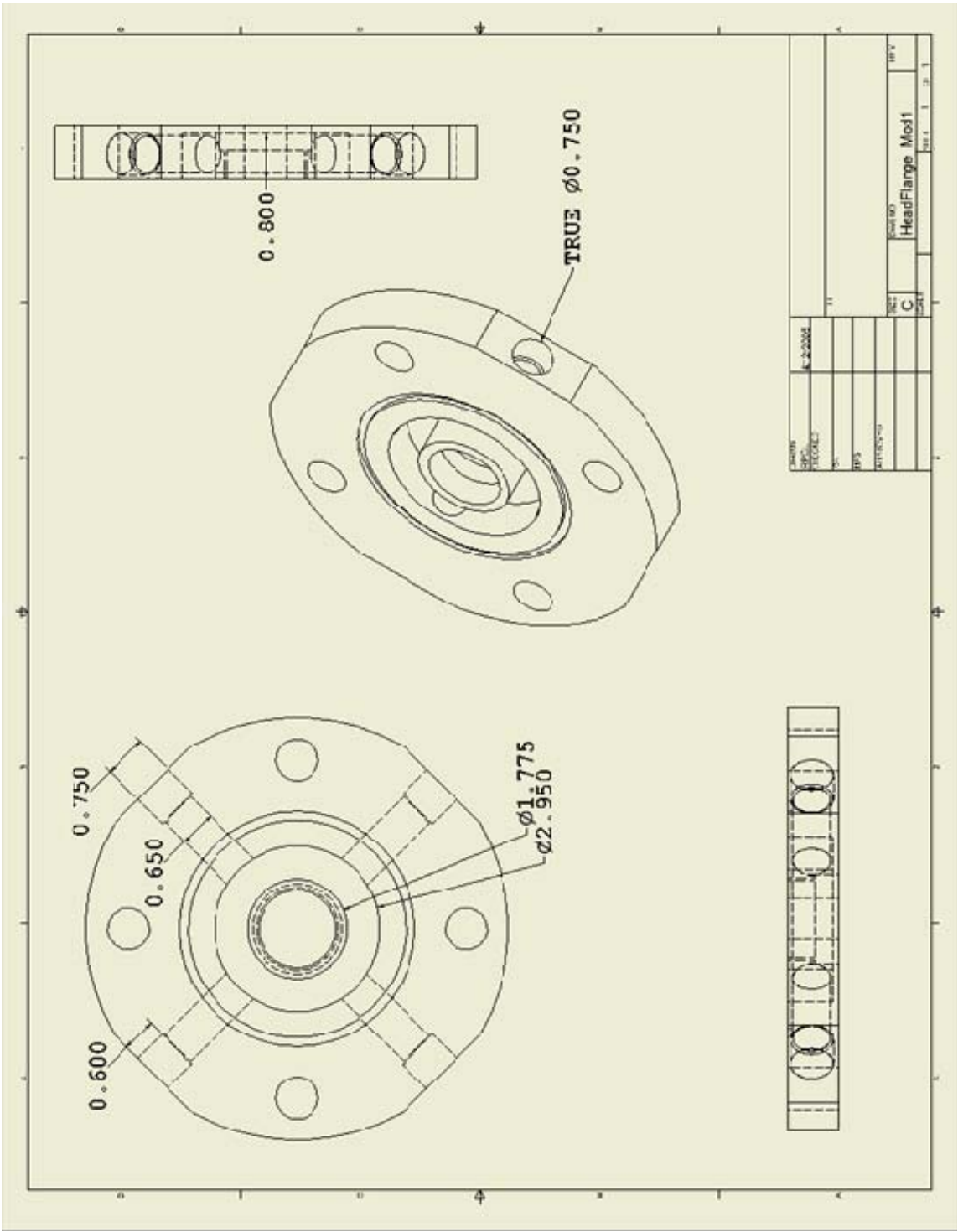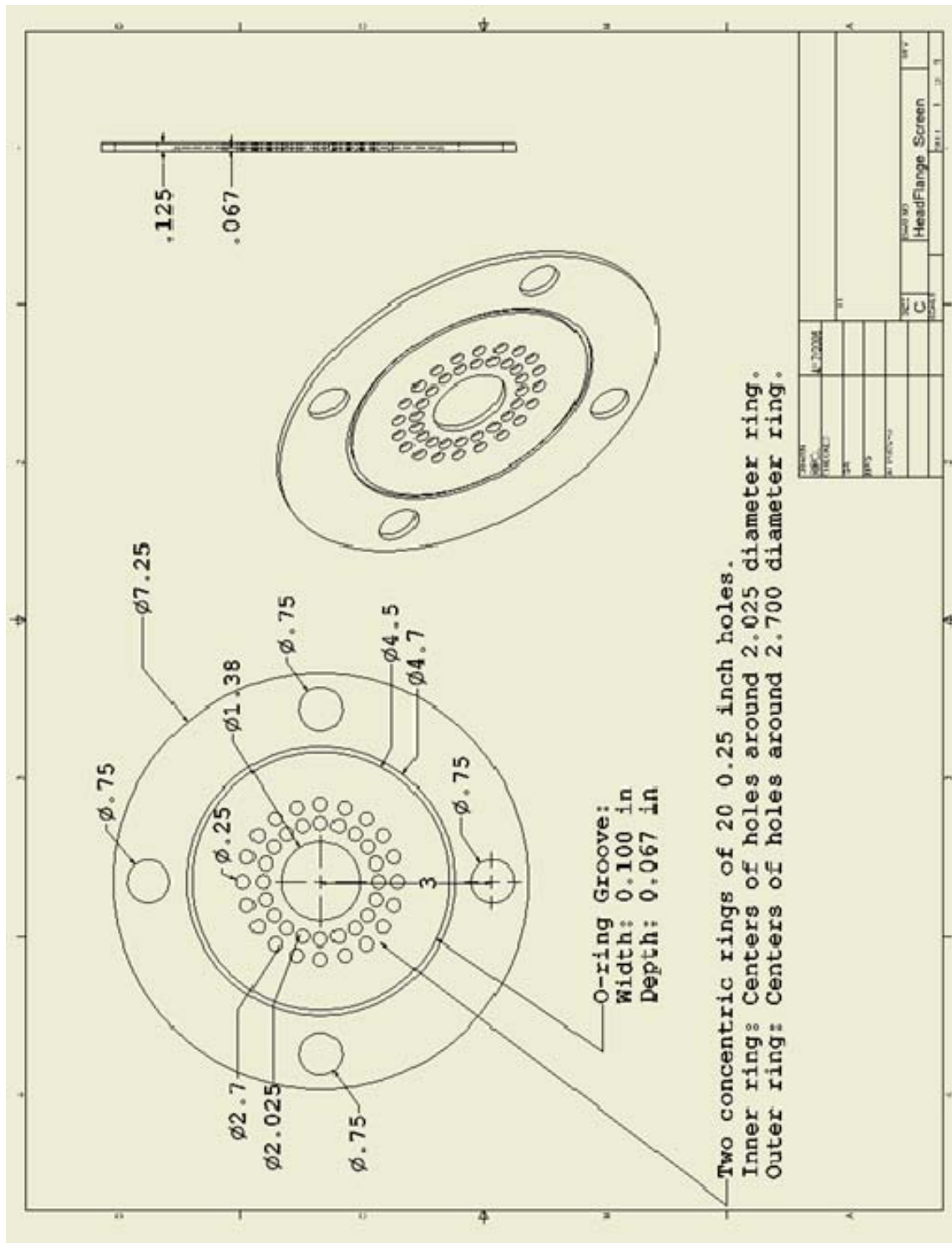Figure 30.   Head Flange Modifications

Figure 31.   Flow Conditioning Screen: ¼ Inch Hole Diameter
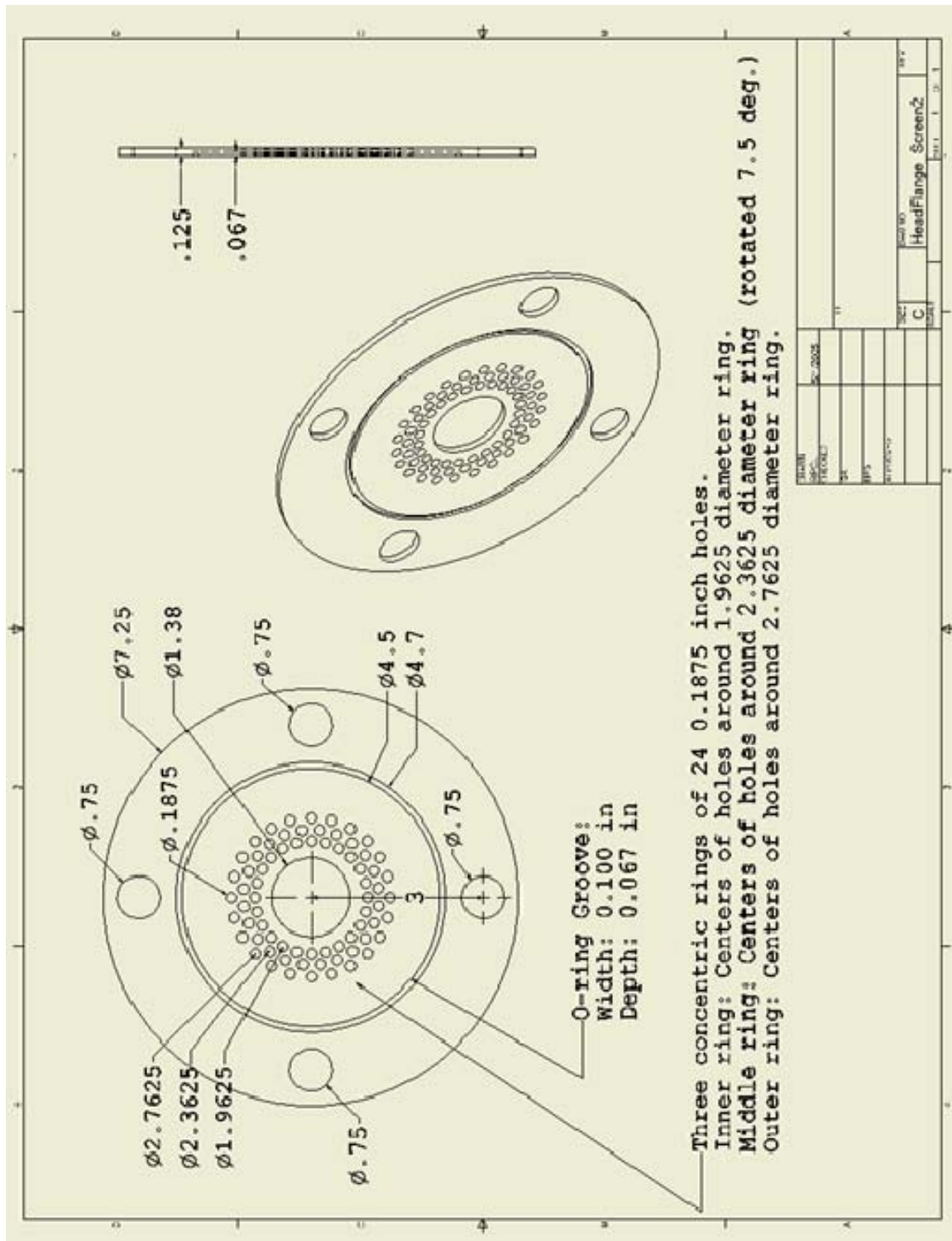
Figure 32.　Flow Conditioning Screen: 3/16 Inch Hole Diameter

THIS PAGE INTENTIONALLY LEFT BLANK

LIST OF REFERENCES

1. Hoffmann, H., "Reaction-Propulsion Produced by Intermittent Detonative Combustion," German Research Institute for Gliding, Report ATI-52365, August 1940.

2. Harris, P.G., Guzik, S.M., and Stowe, R.A., "Design Methodology for a Pulse Detonation Engine as a Ramjet Replacement," AIAA Paper 2004-3400, Joint Propulsion Conference and Exhibit, Ft. Lauderdale, Florida, 11-14 July 2004.

3. Fleeman, E.L., *Tactical Missile Design*, AIAA, 2001.

4. Bussing, T. and Pappas, G. "Pulse Detonation Theory and Concepts," *Developments in High-Speed Vehicle Propulsion Systems,* Progress in Aeronautics and Astronautics, Volume 165, AIAA, 1996.

5. Glassman, I., *Combustion*, Second Edition, Academic Press, Inc., 1987.

6. Kuo, K.K., *Principles of Combustion,* Second Edition, John Wiley and Sons, 2005.

7. Lee, J., "Dynamic Parameters of Gaseous Detonations," *Annual Review of Fluid Mechanics,* Vol. 16, 1984.

8. Shapiro, A.H., *The Dynamics and Thermodynamics of Compressible Fluid Flow,* The Ronald Press Company, 1953.

9. Brophy, C., Sinibaldi, J.O., Wang, F., Jiang, C., and Gundersen, M.A., "Transient Plasma Ignition of a Hydrocarbon-Air Initiator for Pulse Detonation Engines," *Application of Detonation to Propulsion,* Torus Press, 2004.

10. Wang, F., Kuthi, A., and Gundersen, M.A., "Technology for Transient Plasma Ignition," AIAA Paper 2005-0951, *43rd AIAA Aerospace Sciences Meeting and Exhibit,* Reno, Nevada, 10-13 January 2005.

11. Lewis, B. and von Elbe, G., *Combustion, Flames, and Explosions of Gases,* Academic, 1987.

12. Wang, F., Liu, J.B., Sinibaldi, J., Brophy, C., Kuthi, A., Jiang, C., Ronney, P., and Gundersen, M.A., "Transient Plasma Ignition of Quiescent and Flowing Air/Fuel Mixtures," *IEEE Transactions on Plasma Science,* Vol. 33, No. 2, April 2005.

13. Sinibaldi, J.O., Rodriguez, J, Channell, B., Brophy, C., Wang, F., Cathey, C., and Gundersen, M.A., "Investigation of Transient Plasma Ignition for Pulse Detonation Engines", AIAA Paper 2005-3773, *Joint Propulsion Conference and Exhibit,* Tucson, Arizona, 11-13 July 2005.

14. Liu, J.B., Ronney, P., and Gundersen, M., "Corona Discharge Ignition of Premixed Flames", http://carambola.usc.edu/research/coronaignition/coronaignition.html, September 2005.

15. Rodriguez, Joel, "Investigation of Transient Plasma Ignition for a Pulse Detonation Engine." Master's Thesis, Naval Postgraduate School, Monterey, California, March, 2005.

16. Benedict,R.P., Fundamentals *of Temperature, Pressure, and Flow Measurements,* John Wiley and Sons, 1984.

17. Brophy, C.M., Sinibaldi, J.O., Ma, L., and Klingbeil, A.E., "Effects of Non-Uniform Mixture Distributions on Pulse Detonation Engine Performance,' AIAA Paper 2005-1304, *43rd AIAA Aerospace Sciences Meeting and Exhibit,* Reno, Nevada, 10-13 January 2005.

INITIAL DISTRIBUTION LIST

1.   Defense Technical Information Center
        Ft. Belvoir, Virginia

2.   Dudley Knox Library
        Naval Postgraduate School
        Monterey, California

3.   Dr. Gabriel Roy
        Office of Naval Research
        Arlington, VA

4.   Professor Christopher Brophy
        Department of Mechanical and Astronautical Engineering
        Naval Postgraduate School
        Monterey, CA

5.   Professor Jose O. Sinibaldi
        Department of Mechanical and Astronautical Engineering
        Naval Postgraduate School
        Monterey, CA

6.   Dr. Martin Gundersen
        University of Southern California
        Los Angeles, CA

7.   LCDR Brent Channell
        Naval Postgraduate School
        Monterey, CA